

https://dspace.org/

Application of discrete fracture network model to rockfall analysis at Jwaneng Mine, Botswana

Kebatsetse, Lesego Queen

2021
https://hdl.handle.net/10539/33346

Downloaded from a DSpace repository. https://dspace.org/

UNIVERSITY OF THE
WITWATERSRAND,
JOHANNESBURG

APPLICATION OF DISCRETE FRACTURE NETWORK MODEL TO ROCKFALL ANALYSIS AT JWANENG MINE, BOTSWANA

Student Name:	Lesego Queen
Student Surname:	Kebatsetse
Student number:	1778688
Supervisor:	Prof R. Mitra

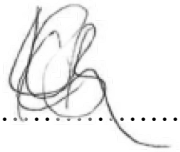
MSc (50/50)	MSc by Research only	PhD
X		

A research report submitted to the Faculty of Engineering and Built Environment, University of the Witwatersrand, Johannesburg, in partial fulfilment of the requirements for the degree of Master of Science in Engineering

August 2021

DECLARATION

I, Lesego Queen Kebatsetse, do hereby proclaim that this research project is my own original work and that all references have been acknowledged. This work has never been submitted for any qualification at any university.



…….. 31/08/2021 ……..

Lesego Queen Kebatsetse Date

ACKNOWLEDGEMENTS

I would like to acknowledge and appreciate the advice and guidance of my Debswana colleagues, and managers, Wits supervisors and industry experts who were essential in the completion of this research report. The following deserve a special mention: Prof Rudrajit Mitra for ensuring that this report satisfies the Wits and international academic requirements, Dr Marc Elmouttie for his assistance in constructing a DFN model and Dr Lesego Kgotlhang & Abel Tunono for their coaching and sponsorship. For the time and energy, you both put in editing and advising to ensure a professional written and presented research report, I thank you.

I am also grateful to the Debswana – Jwaneng Mine for allowing me to carry out my research using the organisation as a case study. My greatest appreciation goes to the staff members of Jwaneng Mine for their support and cooperation during the data gathering process. Percy Matlhabaphiri deserves a special mention for the mine survey assistance.

Last but certainly not least, I would also like to thank my family, my kids: Alpha, Eunice and Ryan for understanding when I could not spend time with them whilst working on the research report. Most importantly, I am thankful to my husband Kebatsetse Otukile for encouraging me to tread on when it seemed I would not make it.

ABSTRACT

Jwaneng open pit mines kimberlite pipes that intruded within the Karoo Supergroup sedimentary deposits in south-east Botswana. The western Cut 7 walls of the mine have an elevated risk of rockfalls. Rockfalls are a leading cause of fatalities in both open pit and underground mine operations. There is a need to quantify rockfall risks so that appropriate and adequate management plans are developed to ensure safe mining. Currently Jwaneng mine uses DIPS RocScience software for rockfall and kinematic analysis. It has been observed that DIPS is inadequate in the required statistical analysis of rockfalls since it does not consider all attributes of fractures. In this RocScience software, attributes of fractures that are considered are orientation and spatial distribution only. Therefore, this assessment excludes other fracture attributes that are important in rockfall analysis such as length, termination, radius and intensity.

To address this deficiency, a DFN model was constructed using the SiroModel software. The DFN model was used for rockfall statistical analysis of the Jwaneng Mine Cut 7 walls at bench scale. The DFN model results showed current 90° bench design is not optimal for the Cut 7 walls. This design angle results in elevated risks of rockfalls. A majority of the potential rockfalls, 90% of the population will have volumes between $1m^3$ and $10m^3$. A 75° bench angle is identified from the model as the optimal bench angle in the research area. This angle is recommended for implementation on the Cut 9 walls because numerous historic data collection projects, have shown that the Cut 9 walls have the similar structural fabric as the Cut 7 walls therefore findings can be postulated across these walls.

Table of Contents

DECLARATION ..... **i**

ACKNOWLEDGEMENTS ..... **ii**

ABSTRACT ..... **iii**

List of Figures ..... **vii**

List of Tables ..... **ix**

Abbreviations & Symbols ..... **x**

Definitions ..... **xi**

1 INTRODUCTION **1**

1.1 Introduction 1

1.2 Purpose of Research 2

1.3 Problem Definition 3

1.4 Research Objectives 4

1.5 Assumptions 4

1.6 Chapter Overview 4

2 GEOTECHNICAL SETTING **6**

2.1 Jwaneng Mine Background 6

2.1.1 Lithology and Geological Structure of Jwaneng Mine 7

2.1.2 Geotechnical Domains of the Jwaneng Open Pit 11

2.2 Chapter Summary 12

3 LITERATURE REVIEW **13**

3.1 DFN Overview 13

3.2 Data Collection and Validation 14

3.2.1 Orientation Bias 15

3.2.2 Size Bias 15
3.2.3 Truncation Bias 16
3.2.4 Censoring Bias 16
3.3 DFN Model Generation Process 16
3.3.1 Fracture Spatial Model 17
3.3.2 Fracture Orientation 19
3.3.3 Fracture Terminations 20
3.3.4 Fracture Length Distribution 20
3.3.5 Fracture Size/Radius 21
3.3.6 Fracture Intensity 21
3.4 SiroModel Software 22
3.5 SiroModel DFN Application to Open Pit Mines 23
3.6 Chapter Summary 23
4 RESEARCH METHODOLOGY 25
4.1 Selection of a Research Area 25
4.2 Data Collection and Manipulation 26
4.2.1 Laser Scanning – Survey Positioning 26
4.2.2 Laser Scanning – Data Collection 29
4.2.3 Maptek PointStudio 8 Structural Mapping 31
4.3 Analysis of Fracture Sets Attributes 33
4.3.1 Fracture Orientation 33
4.3.2 Fracture Spacing 34
4.3.3 Fracture Length Distribution 35
4.3.4 Fracture Terminations 36
4.3.5 Kinematic Analysis 36

4.3.6 Planar Failure 37
4.3.7 Wedge Failure 39
4.3.8 Toppling Failure 40
4.4 Chapter Summary 41
5 DFN MODEL BUILDING AND CALIBRATION 42
5.1 Calibration of the DFN Model 43
5.1.1 Fracture traces Calibration 43
5.1.2 Stereoplot Calibration 44
5.1.3 Kinematic Analysis Calibration 45
5.2 Chapter Summary 47
6 RESULTS AND ANALYSIS 48
6.1 Block Model Analysis 50
6.1.1 Effective Face Angle 50
6.1.2 Back Break Analysis 50
6.1.3 Crest Damage Analysis 51
6.1.4 Block Volume Analysis 52
6.2 Chapter summary 54
7 CONCLUSIONS AND RECOMMENDATIONS 55
7.1 Conclusions 55
7.2 Recommendations 56
REFERENCES 58

List of Figures

Figure 1: Jwaneng Mine open pit expansion – split shell open pit expansion 6
Figure 2. Locality map, showing the distribution of the major subdivisions of the Transvaal Supergroup 7
Figure 3: The three deformation events observed in Jwaneng Mine 10
Figure 4. Chronology of Jwaneng geotechnical domains with structural model update 11
Figure 5: T-type and X-type termination 20
Figure 6: Research area 25
Figure 7: Jwaneng Mine Survey Control Network 27
Figure 8: Jwaneng Mine Survey Beacon 28
Figure 9: The Maptek I-Site 8820 Laser Scanner 29
Figure 10: Cut 7 wall image produced from Maptek Maptek I-Site 8820 31
Figure 11: The settings on the automatic mapping tool 31
Figure 12: Cut 7 wall mapped fracture sets 33
Figure 13: Stereographic plot of mapped Fracture Sets (planes and poles) 34
Figure 14: Fracture spacing distribution per Fracture Set 35
Figure 15: Fracture length distribution per set 36
Figure 16: Geometry of plane slope failure: 37
Figure 17: Cut 7 walls Planar failure analysis stereographic projection from Maptek I-site software 38
Figure 18: Geometry of wedge slope failure 39
Figure 19: Cut 7 walls wedge failure analysis 40
Figure 20: Geometry of toppling failure 40
Figure 21: Cut 7 walls toppling failure analysis 41
Figure 22: SiroModel fracture traces calibration 43
Figure 23: SiroModel stereoplot data calibration 44
Figure 24: Stereoplot comparison of Simulated fractures and mapped fractures 45
Figure 25: SiroModel failure mode calibration 46
Figure 26: Monte Carlo simulations 48
Figure 27: Block simulated from the four mapped fracture sets 49
Figure 28: Block model simulations from the three stochastic fracture sets 49

Figure 29: Effective face angle analysis of the research area 50
Figure 30: Back break analysis of the research area 51
Figure 31: Total crest damage analysis..... 52
Figure 32: Potential rockfall block volume distribution within the study area 52
Figure 33: Block location analysis of the 100 Monte Carlo simulations 53
Figure 34: Potential rockfall Hazard Map of the research area 54

List of Tables

Table 1. Kanye Basin sequence 8
Table 2. Stratigraphic Sequence of the Jwaneng country rock 9
Table 3: DFN model properties 16
Table 4: Main review of the DFN model applicability 18
Table 5: Summary of failure percentage per failure mode on the study area 37
Table 6: Research Area DFN Model inputs 42

Abbreviations & Symbols

DFN – Discrete Fracture Network

ALARP – As Low as Reasonably Possible

PDFs – Probabilistic Density Functions

OPS – Open Pit Simulator

CSIRO – Commonwealth Scientific and Industrial Research Organisation

GNSS – Global Navigation Satellite System

m – metre

Definitions

Rockfall – refers to rock failures and potential rock failures that are less than a bench in size. The rock failures must be defined by interaction of natural fractures in rock (joints, bedding and faults).

Fracture – any geological structures (joints, bedding, faults)

Bench width – the horizontal width of a bench measured from the toe of the preceding bench to the crest of the bench of interest in open pit mining configuration.

Geo-referencing – the process of assigning real-world coordinate to each pixel of the raster. In the case of this research, georeferencing was achieved by assigning Jwaneng mine local coordinates to pixels obtained using a Maptek laser scanner.

Back-break – refers to the distance away from the original crest moved by the degraded crest moves damage, Ryan and Pryor (2000).

DFN Standard – is a wedge type analysis, but still based on the 3D DFN. For this analysis, processing options include daylight vector test mode, maximum angle to classify plane failures and minimum joint radius to be considered.

DFN Polyhedral – considers the analysis of arbitrarily shaped blocks. The potential failure of blocks is based on computation between resisting and driving forces. Resisting forces of a block include its surface properties and engineered resistance. The driving forces, that may result in a block failure are weight, static forces and pore pressure.

1 INTRODUCTION

1.1 Introduction

Mine design, rock engineering and mine implementation practices takes place in an environment of considerable uncertainty. This uncertainty is a result of the unpredictable behaviour of rock masses. The unpredictable behaviour of rock masses is a direct consequence of the variability within the rock mass. This unpredictable behaviour of rock mass lead to rockfalls and slope failures. Rockfalls are a leading cause of fatalities in both open pit and underground mining operations. The uncertainty needs to be quantified and managed at the mine design stage. One way of quantifying this uncertainty is by using probabilistic failure prediction methods. It has been noticed that rock slope failure mechanisms have become more complex with the deepening of open pit mines. Failure of such large open pit mines is a complex combination of slip and/or opening of natural fractures, small non-persistent fractures and failure through intact rock, leading to what is termed as step-path slope failure mechanisms (Brideau, *et al.*, 2009).

Currently, the most common stability analysis methods are limit equilibrium and kinematic analysis. The limit equilibrium stability analysis method assumes continuous slip planes and a known failure mechanism. However, this assumed knowledge of the location and mode of failure mechanisms may result in over or under conservative design recommendations. The kinematic analysis on the other hand does not consider all attributes of fractures; it only uses fracture orientation. This method ignores other attributes such as fracture length, fracture condition and intensity. The method also assumes infinite continuity of fractures. Similar to the limit equilibrium method, this may result in over or under conservative design recommendations.

A Discrete Fracture Network (DFN) is defined by Lei, *et al*. (2017) as a computational model that explicitly represents the geometrical properties of each fracture, and the topological relationships between individual fractures and fracture sets. DFN models offer the opportunity to take into account variability due to joint geometrical properties. Stochastic simulation of fracture systems is the geometric basis of the DFN approach and plays a crucial role in the performance and reliability of DFN models (Jing & Stephason, 2007). Probabilistic density functions (PDFs) are used to describe geometrical parameters of fracture sets related to the density, location, orientation

and size, based on the collected geotechnical data (Balzarini, *et al.*, 2001 as cited in Jing & Stephason, 2007).

The validity and accuracy of any DFN model are heavily dependent on the data collection practices followed. Published data collection best practice must be followed to ensure that the output DFN model produced closely represents reality (Miyoshi *et al*., 2017). Thus, the research will follow the data collection best practices and build a DFN model from the collected data. The DFN model will then be used for statistical analysis of rockfalls. The minimum and maximum predicted rockfall sizes will be recommended for use in the mine to determine minimum and maximum bench catchment capacity requirements.

1.2 Purpose of Research

Jwaneng Mine started a new pushback (Cut 9) at the start of 2019 on the western part of the open pit. Overall slope stability geotechnical risks on this part of the open pit are as low as reasonably possible (ALARP). The main contributing factor to this ALARP state of slope instability is the favourably oriented bedding. Bedding on the western side of the pit dips into the wall. However, the probability of rockfall risk remains elevated. The rockfall risk is elevated by the numerous interactions of existing joint sets, faults and bedding planes. The maximum size of the expected rockfall is therefore the single most important factor that determines the size of the designed catchment area. Rockfall in the context of this research refers to rock failures and potential rock failures that are less than a bench in size. The rock failures must be defined by the interaction of natural fractures in rock (joints, bedding and faults).

On the western wall of the pit, Jwaneng Mine is currently exploiting Cut 7. From the various exploration regimes undertaken, geology and structural geological conditions are expected to be similar between Cut 7 and Cut 9. The researcher will therefore use Cut 7 as a case study and apply learnings to the Cut 9 walls.

The researche seeks to use a DFN model to determine the possible minimum and maximum rockfall sizes that result from the interaction of the natural fractures. A DFN model is deemed to be the best methodology for conducting this research because they (DFNs) are a probabilistic

representation of potential rock failure behaviour. Due to its probabilistic nature and incorporation of structural properties, the DFN has been proven to be a suitable method for representation of structural uncertainty in rock masses. The use of the DFN model for this analysis is expected to improve the accuracy of design recommendations and statistical rockfall risk predictions.

1.3 Problem Definition

Jwaneng Diamond Mine's western slopes have an ALARP state for the overall slope stability. However, these western slopes have an elevated risk of rockfalls. Current slope monitoring techniques such as terrestrial radars are not capable of proactively detecting potential rockfalls which places personnel and equipment at unacceptable levels of risk. Developing an accurate representation of the rock mass fabric is a key element in a rock fall hazard. Well calibrated models (using an optimal number of fracture properties) can be used to 'predict' potential rockfalls.

The mine currently uses stereographic projection for statistical analysis of rockfalls. This technique utilises orientation data (dip and dip direction) of natural fractures/geological structures (joints, faults and bedding) that have been mapped. The stereographic projection supports analysis of possible failure mechanisms (that is planar, wedge, toppling or circular failure type) that are most likely to occur from the interaction of the plotted geological structures. However, the stereographic projection technique has the following limitations:

- It does not consider the physical location of structures in relation to one another. Thus, it may predict interaction on geological structures that are many kilometres apart and do not have sufficient persistence to ever interact with one another;
- It assumes an infinite continuity/persistence of all fractures that are being analysed. This may over-estimate the number of possible failures from the interaction of the analysed structural failures; and
- This method also ignores all other fracture properties that are important in determining the strength and failure susceptibility of a fracture. Properties that are not considered when using stereographic projection include fracture length, fracture intensity, spatial variation and termination percentage.

This research seeks to use DFN modelling for statistical analysis of rockfalls in Jwaneng Mine. Numerous authors including Elmo *et al*. (2015) have proved that DFN modelling can overcome many of the above-identified limitations of stereographic projections.

1.4 Research Objectives

A DFN model is arguably a superior tool for rockfall analysis. The goal of this research is to interrogate a constructed DFN model for rockfall risk identification and quantification so that appropriate mitigation is recommended. To achieve this, the objectives of the research are as follows:

- To construct a DFN model using the OPS SiroModel software;
- To conduct a statistical rockfall analysis from a constructed DFN model;
- To compare results from a stereographic projection and DFN model where possible; and
- To recommend improvements to bench designs in Jwaneng Mine where applicable.

1.5 Assumptions

The following assumptions will be made in this research work;

- The chosen method of data collection – that's is laser scanner mapping has acceptable error limits and will therefore yield data of acceptable quality;
- The chosen modelling software (OPS SiroModel) has acceptable limitations; and
- Near-surface analysis is being considered. Dry bench conditions exist near-surface and thus there will be no pore pressure considerations in the model.

1.6 Chapter Overview

In this report, Chapter 2 gives the background of the study area that includes; the geographical setting of Jwaneng Mine, the geological as well as the geotechnical setting of Jwaneng Mine as reviewed from the available literature. The geotechnical review of Jwaneng Mine presents a deficiency that is to be addressed by this research. Chapter 3 is a presentation of currently available

literature on DFN modelling. This chapter is not provided as a complete reference to DFN modelling. Rather, the chapter provides summaries on DFN literature, DFN model data requirement and DFN model building process. Chapter 4 is the research methodology chapter that presents the method of data collection utilised as well as the collected data. This chapter also provides the reader with quality assurance and quality control protocols that were employed to ensure that data is compliant to set industry standards. The research methodology chapter also provides analysis of collected data. The analyzed data forms an input into the DFN modelling, which is the objective of this research project. Chapter 5, the DFN model building and calibration chapter, is a summary of inputs into the SiroModel software. The chapter also discusses the various calibration processes that were undertaken to ensure that the model simulation correctly represents field observations. SiroModel block model results and analysis are presented in Chapter 6. The block model was generated from one hundred Monte Carlo simulations. Adequacy of the one hundred Monte Carlo simulations was tested by ensuring that they fill the histogram. Chapter 7 presents the conclusions and recommendations based on this research.

2 GEOTECHNICAL SETTING

2.1 Jwaneng Mine Background

Jwaneng Diamond Mine is located in the southern part of Botswana which is approximately 160 km from Gaborone along the Kanye-Ghanzi highway. On the grid reference the mine lies between S024.30º S024.7º and N 024.30º N024.58º. The geomorphology of the Jwaneng area is relatively flat and can be accessed by vehicles (Debswana, 2018).

Jwaneng Mine is a 50/50 joint venture between the Government of Botswana and the DeBeers Group of Companies. This mine is the largest diamond producer by value in the world (Debswana, 2018). The Diamond mine utilises split shell pushbacks, that is, a new open pit pushback is undertaken on only half of the existing open pit along the open pit long axis. The split-shell pushbacks are done on the eastern and western sides of the open pit alternatively along the long pit axis as shown in Figure 1. A vertical section through the various open pit expansions is also shown on this Figure 1.

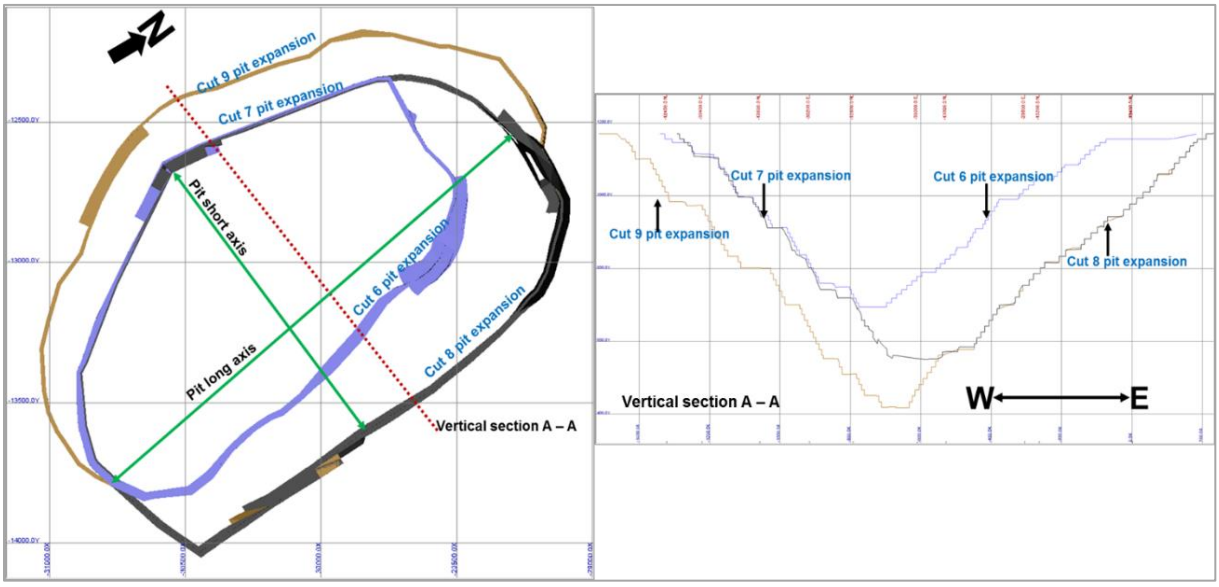


Figure 1: Jwaneng Mine open pit expansion – split shell open pit expansion adapted from (Debswana, 2017)

The current open pit has dimension of width of 1.7 km (pit short axis), length of 2.5 km (pit long axis) and depth of 400 m. The current pushback on the eastern side of the pit, Cut 8, is expected to extend the life of mine to year 2029 and depth of 652 m. The mine began excavation of Cut 9 in January 2019. This pit expansion is scheduled to start ore extraction in 2029 and extend the life of the mine by another 5 years to 2034 to a depth of 823 m (Debswana, 2017).

2.1.1 Lithology and Geological Structure of Jwaneng Mine

According to Moore, *et al.* (2001), the Transvaal Supergoup is a late Archaean to early Proterozoic succession of meta-sediments within the Kaapvaal Craton. It contains three unconformity bounded sequences. The base of these three unconformity bounded sequence is typically the basal quartz arenites, overlain by the dolomite and the iron formations form the roof. The detailed lithostratigraphy is shown in Figure 2.

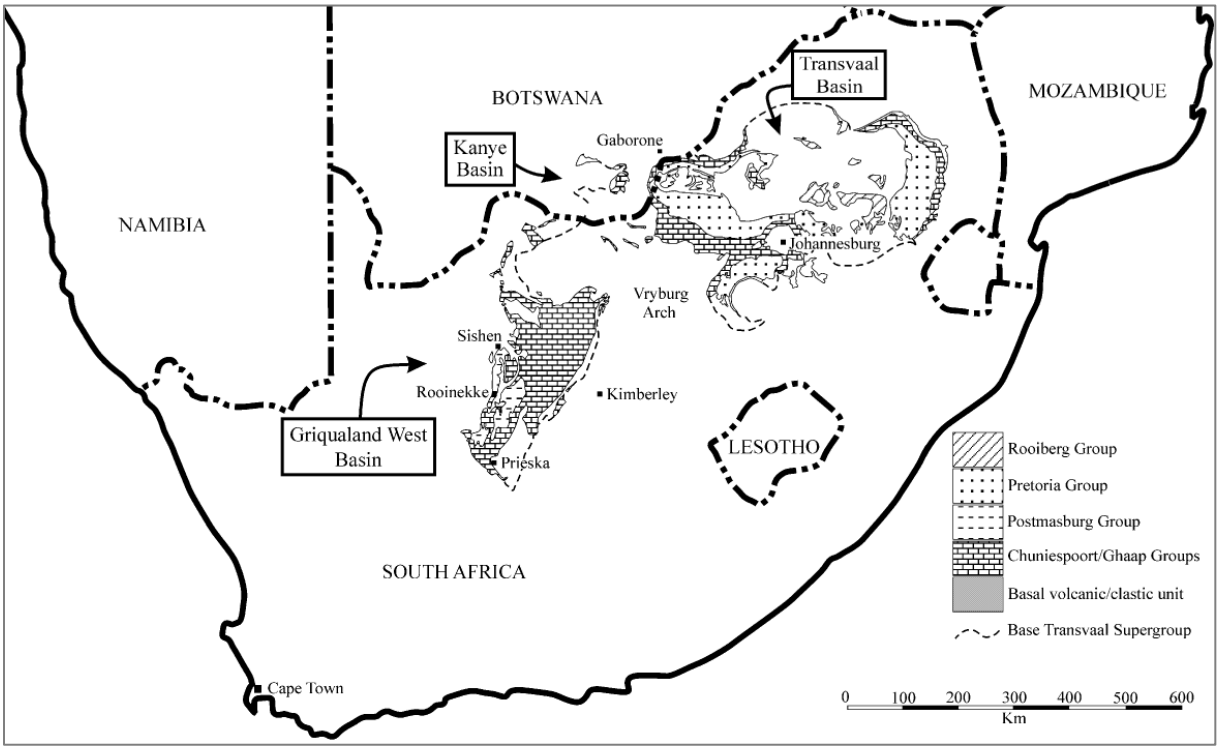


Figure 2. Locality map, showing the distribution of the major subdivisions of the Transvaal Supergroup (adapted from Moore *et al.*, 2001)

The Transvaal Supergroup is preserved in two different geographic locations - the Transvaal Basin and the Griqualand West Basin. The Griqualand West Basin seats on the western margin of the Kaapvaal craton that extends into South-East Botswana as part of the Kanye Basin. Jwaneng Mine is part of the Kanye Basin sequence (Moore, et al., 2001).

According to Mapeo and Wingate (2009), the Kanye Basin sequence has the Taupone dolomites as its base, overlain by the Segwagwa Group sequences. The Rooiberg Group which is present in the Transvaal group have been eroded and are not present within the Kanye Basin. The detailed lithostratigraphy of the Kanye Basin is shown in Table 1. This table, adapted from Mapeo & Wingate (2009), also shows the description and ages of the different formations within the Kanye Basin.

Table 1. Kanye Basin sequence (adapted from Mapeo and Wingate, 2009)

Group	Formation	Description	Age
	Segwagwa-Masoke	Granite, diorite, syenite	2054 ± 9 Ma (this paper) (SHRIMP on zircons, granite emplacement age)
	Moshaneng	Granite, diorite, syenite	2054 ± 2 Ma (Mapeo et al., 2004a) (U–Pb on zircons, granite emplacement age)
	Intrusive contact		
	Lomugau	Sandstone, quartzite	
	Monotoholwane	Sandstone, quartzite	2193 ± 20 Ma (Mapeo et al., 2006a) (SHRIMP on zircons, detrital)
Segwagwa	Gatsepane	Shale, chert	
	Mogapinyana	Iron rich shale, orthoquarzite, sandstone	2236 ± 13 Ma (Mapeo et al., 2006a) (SHRIMP on zircons, detrital)
	Tsatsu	Basalt, andesitic lavas, diabase	
	Tlaameng	Shale, chert clast conglomerate	
	Ditojana	Shale, siltsones, ferruginous sandstone	2250 ± 14/15 Ma (Mapeo et al., 2006a) (SHRIMP on zircons, detrital)
	Unconformity		
	Kgwakgwe Chert Breccia	Chert breccia	
	Masoke Ironstone	Banded ironstones	2431 ± 31 Ma (Trendall et al., 1990) (U–Pb on zircons: volcanic unit, emplacement age)
Taupone Dolomite	Ramonnedi	Dolomite, chert	
	Black Reef Quartzite	Conglomerate, arenite, tuff and shale	2642 ± 3 Ma (Walraven and Martini, 1995) (Pb-zircon evaporation, tuff bed emplacement age)

Jwaneng Mine exploits three main diamondiferous kimberlite pipes which have intruded a sedimentary sequence. The mine lies on the Kanye Basin, which is situated on the Pretoria Group of the Transvaal Supergroup that was set in the Proterozoic period. The diamondiferous kimberlitic pipes have intruded a succession of sedimentary rock formations of shale and dolomite. Dolerite sills and dyke also intrude the country-rock. The strata surrounding the mine varies between dips of 10˚ - 40˚ towards the northwest (Barnett, 2008).

According to Barnett (2008), the Jwaneng stratigraphic sequence begins with the Kalahari sequence, which is comprised of sand and calcrete, which is then underlain by a succession of shales. A chert pebble conglomerate horizon locally termed bevets acts as a marker bed within the quartzitic shales. The dolomite which has variable thickness, forms the base rock for the Jwaneng stratigraphic sequence. The Jwaneng stratigraphic sequence is shown in Table 2.

Table 2. Stratigraphic Sequence of the Jwaneng country rock (adapted from Barnett, 2008)

Typical Thickness (m)	Rock Type	Rock Code
15-20	Sand	Sand
40	Calcrete	Calcrete
Residual	Laminated Shale	LS
30	Carbonaceous Shale	CS
135	Quartzitic Shale	QS
0-4	Bevets	BVT
Variable	Dolomite	DM

Numerous authors including Mapeo & Wingate (2009) and Creus, *et al*. (2018) accept that the Transvaal Supergroup, as observed in Jwaneng Mine, which is a part of Kanye Basin have undergone three deformational events. The three deformational events are discussed below:

> *"a. An early compressional, NW-SE, fold-and-thrust event resulted in, firstly, development of low-angle thrusts, followed by NE-trending, open F_1 folds. A diverging fanning axial planar cleavage formed around these open F_1 folds, that broadly trends NE.*
>
> Analysis by Creus *et al*. (2018) suggest that the D2 deformation event occurred in two stages:
>
> *b. D2 is inferred to be a progressive deformational event in which there was clockwise rotation of the maximum principal stress from NW-SE direction to a NE-SW direction. The first stages of this deformational event resulted in oblique, left lateral shearing along pre-existing cleavage planes around F_1 folds. Locally, reactivated cleavage planes merged with*

thrust planes to form rotated half-grabens. Shearing along the NE-trending cleavage was accompanied by the development of antithetic structures.

c. The latter stages of D2 saw the resolution of strain by further folding. The principal stress direction would have been NE-SW, resulting in the formation of open, broad, NW trending F2 folds. A weakly-fanning cleavage planes developed around F2 folds.

d. The dominant structures at Jwaneng Mine are normal faults that exploited pre-existing structures during NW-SE extension. The dominant fault set is NE-trending and exploited cleavage around F1 folds. Subordinate faults terminate against NE-trending faults, and exploited antithetic structures and cleavage around F2 folds. This network of faults created a series of "diamond- or rhomboid-shaped" blocks with variable rotation within each block, especially at termination points of N-trending and NW-trending faults," (Creus, et al., 2018).

Figure 3 is a pictorial representation of the three deformational events as interpreted by Creus, *et al*. (2018) in Jwaneng Mine.

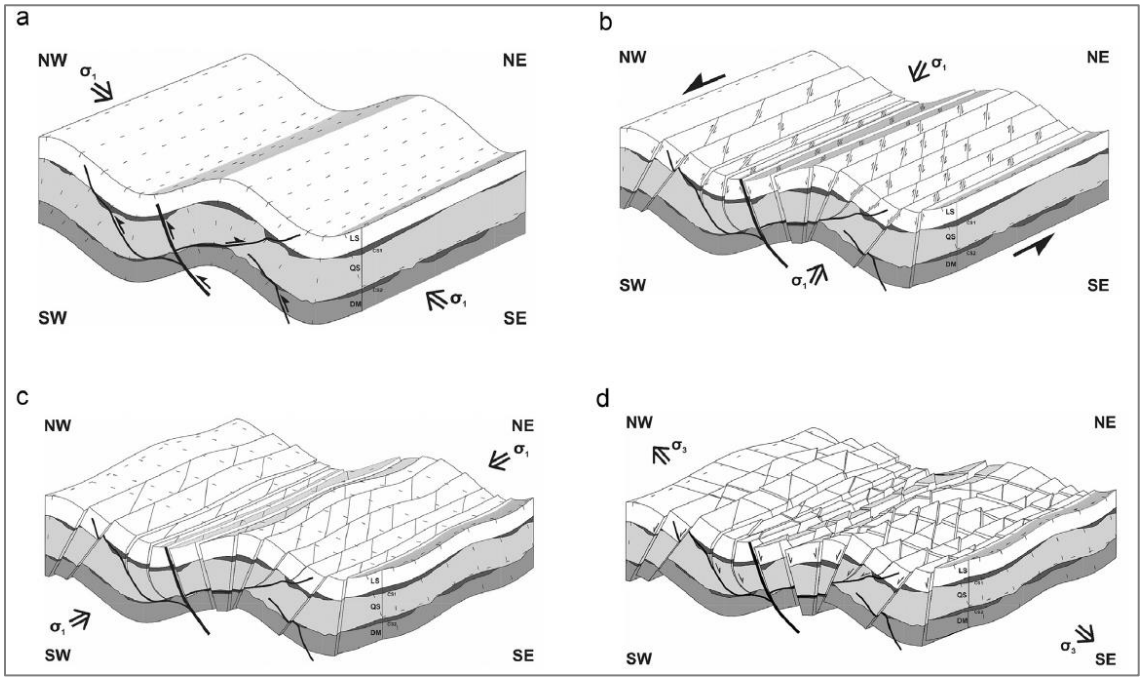


Figure 3: The three deformation events observed in Jwaneng Mine adapted from Creus *et al*. (2018)

2.1.2 Geotechnical Domains of the Jwaneng Open Pit

The first known structural model of Jwaneng Mine was developed by Dirks (2001). As new better and technologies for data collection and analysis are developed, the structural model of Jwaneng Mine is continuously reviewed and updated to reflect the new structural picks. The reviews are undertaken by the mine with expert advice from various consulting groups which include SRK, TECT and ITASCA.

The major structures which are dominantly NE – SW striking faults are used to define the geotechnical domains. These faults are down-thrown to the southeast and compartmentalise the shallow to intermediate northwest dipping strata into domains, which are the aforementioned geotechnical domains. Figure 4 shows the major changes in the definition/identification of geotechnical domains that resulted from structural model updates over time.

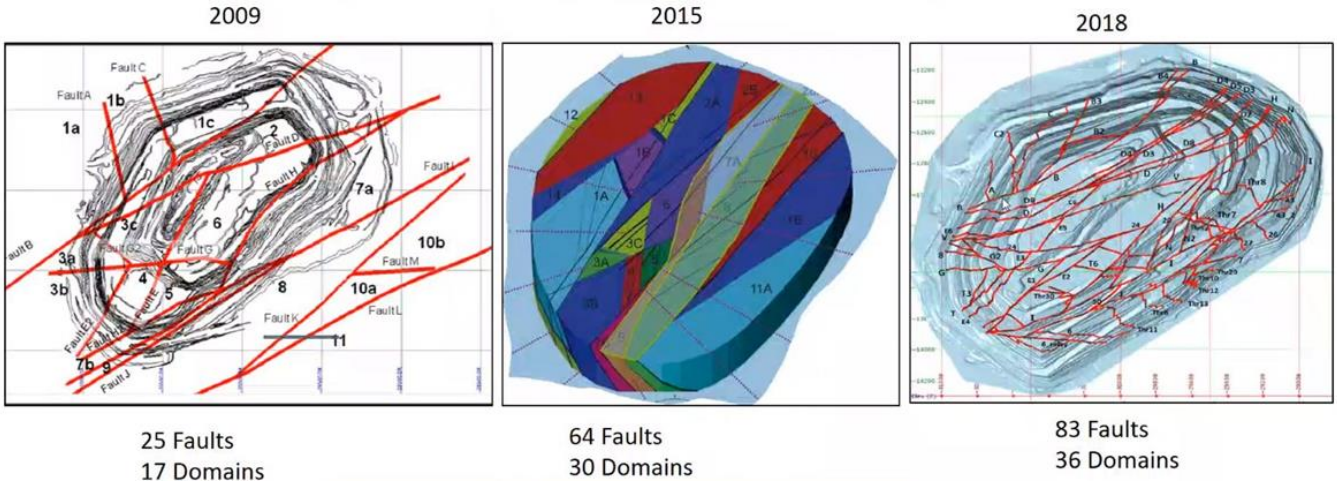


Figure 4. Chronology of Jwaneng geotechnical domains with structural model update

In using the dip of strata to define the geotechnical domains, Jwaneng structural model updates turn to focus more on the bedding. This biased focus on bedding resulted in minimal analysis of other finite fractures such as joints. The limited research on joint interaction increased significantly with the mining of Cut 8 on the eastern half of the Jwaneng open pit. Bedding on the eastern side

of Jwaneng Mine daylights into the open pit and has been identified as the major controlling factor for open pit stability overriding the non–discontinuous jointing within the slope.

Jwaneng Mine the started mining of Cut 9 in January 2019. This cut is on the western side of the Jwaneng open pit. Available research work todate in the Jwaneng open pit has focused on large scale faults and bedding orientation. Bedding on the western side of the open pit is favourable as it dips away from the pit (into the wall). Opportunities for optimization of the Cut 9 open pit shell exist in optimising catchment bench width. Currently, Jwaneng Mine define bench width as per the empirical formulae developed by Call and Nicholas International Mining Consultants. The formulae as shown in Ryan & Pryor (2000) suggests that bench width is estimated by:

$$\boldsymbol{berm\ width\ (m) = 0.2 \times bench\ height + 4.5} \quad \text{..... Equation 1}$$

This is an empirical formula, and since it was not generated with Jwaneng Mine specific data, it does not consider the local site conditions. This research will present a new DFN approach to designing catchment benches by determining rockfall size distribution for the research area. This rockfall size distribution will be provided as a Jwaneng site-specific input to the bench width estimation.

2.2 Chapter Summary

This chapter introduces the Jwaneng open pit expansion methodology – split shell mining. The chapter also covers the lithological and structural setting of Jwaneng Mine within the Transvaal Supergroup. The three deformational events as observed on the Jwaneng Mine stratigraphy are discussed. Jwaneng Geotechnical domains which are defined by the dominantly NE – SW striking faults are discussed. Chapter 2 concludes by showing the criticality of this research in deriving site-specific constants as input into bench design.

3 LITERATURE REVIEW

3.1 DFN Overview

The use of DFN modelling was borne in the early 1970s out of the need to characterise and model fluid percolations in natural fractures (Dershowitz & Einstein, 1988). These studies gained wider practice in the rock engineering fraternity during the 1980s (Xu & Dowd, 2010). According to Grenon, *et al*. (2016), DFNs have found many applications within the mining field. DFNs can be used independently to study structurally defined wedges and unstable blocks. They can also be used for in-depth reseach of rock mass strength when they are embedded within numerical modelling codes.

A DFN is defined as a computational model of rock mass defects that explicitly represents the geometrical properties of each fracture, and the topological relationships between individual fractures and fracture sets (Lei, *et al.,* 2017). According to these authors, a DFN can be generated from geological mapping or geomechanical simulation to represent different types of rock fractures such as joints, faults, veins and bedding planes.

Historically, patterns of fractures have been mapped from the exposure of rock outcrops or man-made excavations to study the process of fracture formation (Pollard & Segall, 1987). More recently, digitised outcrop analogues have been used to build DFNs for numerical simulations (Lei, *et al.,* 2017). Many outcrop-based DFNs have been constructed by various researchers for modelling natural fracture systems (Griffith, 2009). Some terrestrial remote sensing techniques such as photogrammetry were introduced to assist with the mapping of large-scale trace of fractures (Jones, *et al.*, 2016). It is noteworthy that the fracture data collected by a remote sensing method was calibrated by comparing the results with in-situ measurements (Lei, *et al.,* 2017). The outcrop based DFN model has the advantage of preservation of natural fracture features as well as unbiased characterisation of complex topologies.

The stochastic DFN approach applies to both 2D and 3D analyses and it is suitable for application to various scales (Lei, *et al.,* 2017). The key input data for the stochastic DFN model involve deterministic (mapping) and statistical data of fracture length, orientation, location, shape and their

correlation. However, this deterministic/stochastic DFN geometrical representation has some limitations such as uncertainties in statistical parameters and oversimplification of fracture geometries and topologies (Mathis, 2014).

Recent studies on the use of DFN models have shown that the development of hybrid DFN models that assimilate the advantages of both stochastic and deterministic approaches generate better fracture networks that simulate actual geological systems. DFN modelling is increasingly being used in addressing various geotechnical and mining engineering problems (Elmo *et al*., 2014). However, many authors indicate that the success of the DFN approach, as with all modelling, depends on the fracture data quality and quantity available. Thus, the DFN based modelling must take into consideration the fracture data collection techniques used. Statistically rigorous fracture data collection techniques are mostly recommended by the experts of DFN modelling for the model to produce the required results (Mathis, 2014).

3.2 Data Collection and Validation

When conducting data acquisition for DFN modelling, a Geoscientist is required to focus attention on the characteristics of individual discontinuities. Therefore, the DFN based methods can highlight deficiencies and biases that may be present in rock mass sampling programmes that support all downstream geotechnical analyses.

According to Elmo, *et al*. (2015), in DFN modelling structure characteristics including spatial location, intensity, orientation and size are statistically analysed and exploited to create a 3D representation of the rockmass. This maximises the use of structural information thereby providing a near-real representation of the rockmass and its condition.

Different data collection techniques introduce different biases to the collected data. The data has to be corrected for these biases before use. The most common data biases encountered in modelling including DFN modelling are discussed. The applicability of these biases in the current research is also discussed. According to Mauldon (1998), '*the stochastic structures in the DFN should be statistically equivalent to those within the rock mass*,' provided the sampling biases are adequately accounted for.

Zhang and Einstein (2000) identified four (4) possible data errors due to biases associated with data collection methods. The errors are discussed in the following sections.

3.2.1 Orientation Bias

Orientation bias may result in over or under-sampling of certain fracture sets due to the orientation of the mapping direction (data collection) relative to the orientation of the structure. Structures oriented parallel to the mapping direction will be under-sampled (Read and Stacey, 2009). Terzaghi Weighting introduced by Terzaghi in 1965 is the most commonly applied method to correct for orientation bias. This orientation bias correction method has been observed to introduce errors in linear and planar mapping/sampling when the sampling domain is sub-parallel to the existing fractures (Mauldon and Wang, 2006). An angle of 15° has been cited as the minimum angle difference between the sampling domain and the existing fractures for reliable application of Terzaghi Weighting.

For this project, the planar sampling window was sub-parallel to some fracture sets and hence the Terzaghi Weighting could not be applied. The simulated DFN fractures were validated by correlating them to those observed on the rock mass. The correlation was achieved through utilisation of photographs of the research area.

3.2.2 Size Bias

Logically that large joints will be sampled more often than small joints. '*This bias affects the results in two ways: (a) a larger joint is more likely to appear in an outcrop than a smaller one; and (b) a longer trace is more likely to appear in a sampling area than a shorter one*' (Zhang and Einstein, 2000). Size bias is formally accounted for, for assumed joint size distributions using DFN codes based on stereological principles.

3.2.3 Truncation Bias

Truncation, according to Zhang and Einstein (2000), refers to the omission of some fractures from measurement as they are below a certain cut off point. Warburton (1980) suggested a method that can be used for truncation bias correction. For this project, truncation bias on trace lengths was greatly reduced by reduced truncation levels when conducting mapping from laser scanning data. Truncation level was based on empirical analysis of historic rockfalls in the research area.

3.2.4 Censoring Bias

According to Elmo, et al. (2014), censoring bias is introduced in data because long fracture traces cannot be measured due to the limited extent of the rock exposure. Censored fractures have traces that extend beyond the mapping window. Various authors including Priest (1993), Mauldon (1998) and Zhang and Einstein (2000) have discussed in detail ways of correcting this bias to the unbiased trace length of fractures.

As will be presented later, censoring bias is not applicable in the current research because fractures have been assumed to be fully persistent throughout the research area (based on a detailed analysis of the structural mappings for the research area).

3.3 DFN Model Generation Process

Elmo, *et al*. (2015) have suggested the fracture properties required to develop DFN models as shown in Table 3.

Table 3: DFN model properties (adapted from Elmo, et al. 2015)

Primary	Secondary
Orientation distribution	Aperture distribution
Fracture length distribution	Fracture shear strength properties
Fracture intensity distribution	Fracture stiffness properties
Termination percentage	Transmissivity distribution
Spatial variation	Storativity distribution
	Termination percentages

The two columns of properties; primary and secondary show the fracture properties that are required depending on the ultimate use of a DFN model. For all DFN modelling and geomechanical models, only the primary attributes are essential. However, if the DFN is to be used in hydraulic modelling, the secondary attributes will need to be collected over and above the primary attributes. This research will be focused on geomechanical DFN modelling, as thus only the primary fracture properties were collected.

Various authors including Elmo, *et al*. (2015) and Miyoshi, et al. (2017) have outlined a general process for the analysis of a DFN model. According to Miyoshi, et al. (2017), the DFN model requires the input of the structural mapping field data grouped into fracture spatial model, fracture orientation, fracture intensity, fracture size and fracture termination. These inputs are discussed in the following sections.

3.3.1 Fracture Spatial Model

The fracture spatial model defines the way structures are distributed in a 3D space. Spatial models can be defined as either stationary or non-stationary models. The differences in these define "*specific distribution laws used to simulate fracture orientation and fracture location"* (Elmo, *et al*., 2015). Various authors including Dershowitz & Einstein (1988) and Staub, *et al*. (2002) discussed possible models that can be used for defining fracture system models. A summary of the various available methods for simulating fracture spatial model is presented in Table 4 after Staub, *et al*. (2002).

Table 4: Main review of the DFN model applicability (adapted from Staub, *et al*. 2002)

Model	Concept	Applicability	Advantages	Limitations
Orthogonal	Fracture network simulated from 3 sets of unbounded orthogonal joints	rock masses with completely defined rectangular rock blocks / mostly to hydrology	Simple geometry and treatment of data	Planar assumption, limitation in the variation of fracture orientation
Baecher disk	Generate fracture network from fracture centres that are distributed uniformly in space	Homogeneous rocks	Few field data available / Accurate in rock mechanics and hydraulics when a little is known	Do not simulate terminations of fractures, fractures must be planar / Do not account for complex features of fracture populations
Enhanced Baecher	Generate fractures from fracture centres located at random points in space. Intersections are calculated with pre-existing fractures	Fractured rock masses in which joint terminations are observed	Suited for simulation of connectivity of natural fracture population / Multiple intersections per fracture are possible	Fracture size distribution is not preserved; joints must be planar
BART	Same principle as for the Enhanced Baecher model, except that the centre of fracture terminating at intersections is generated from point on fracture intersection	Fractured rock masses in which fracture terminations are observed	Quick simulation / Fracture size distribution is preserved; spatial correlation in the simulated fracture population	fractures must be planar
Veneziano	Fracture network generated in 3 stochastic processes based on Poisson plane and Poisson lines	Suited for 100% persistent and unbounded fractures	Polygonal shapes are often observed in nature. More appropriate than orthogonal model for most cases, specially in case of coplanarity	Often fail to construct blocks / Intersections of fractures do not often match joint edges / Complex 3-D model
Dershowitz	Fracture network generated from 2 stochastic processes based on Poisson plane	Accurate for systems which exhibit distinct rock blocks, bounded polygonal fractures, and orientation dispersion	Model distinct rock blocks of various shape, flexibility in the distribution of fracture orientations / Joint intersection at joint edges	Can generate a large number of smaller polygons / Not so well fitted for coplanar fractures
Mosaic Tessellation	Deterministic and/or stochastic generation of the blocks, then definition of the fracture planes	Fracture systems resulting from a process of block formation (jointing in columnar basalts)	Manage non co-planarity, creation of the blocks first	Not so accurate in cases that do not display polyhedral blocks and polygonal fractures; blocks created first; indirect modelling of location, orientation and shape of fractures
Poisson Rectangle	Same concept as Enhanced Baecher except that fractures are rectangular	Same as Enhanced Baecher	Same as Enhanced Baecher	Specific conceptual model / Require a good knowledge of the rock mass geometry
Geostatistical	Generate fractures according to a specified variogram	Describe the spatial behaviour of regionalised variables of the fracture network	Account for a good spatial correlation	The size of the sampling area must be consequent compared to the study area
War Zone	Simulate higher densities of fractures between two major subparallel fractures	Simulation of fracture network in shear zones and in the surrounding rock mass	Binary model / identify "fracture zone" and "non-fracture zone"	Specific conceptual model / Require a good knowledge of the rock mass geometry
Non-Planar Zone	Generate fractures along a non-planar user defined surface	Simulation of fracture network along specific features (deformation zones,...)	Enhance rock zones with specific geometrical properties / binary model	Require a good knowledge of the rock mass geometry
Levy-Lee Fractal	Generate clusters of smaller fractures around wider fractures	In combination with geostatistical analysis: Hierarchical Fracture Trace Model	Accounts for the chronology of fracture formation / Ability to generate a non-stationary fracture system with a set of parameters that remain constant throughout the generation system	Do not consider the size and shape of the blocks delimited by the simulated fractures / Definition of the most appropriate fractal dimension
Nearest-neighbour	Fractures are organised into primary, secondary and tertiary groups, and are generated in this sequence	Can account for the generation of fracture network according to the theory of fracture genesis	Generate clusters of fractures around the primary group / More explicit than Levy-Lee model if fractures can be classified	Must have enough data to assess the different groups and chronology

According to Elmo, *et al*. (2015), the choice of a specific model for use is dependent on the field data assumptions and geological observations. The Enhanced Baecher model and the BART model have been recognised to be appropriate for use in most general cases. The Baecher model assumes log-normal radii and randomly distributed centroids.

SiroModel uses the Baecher model as the default model. However, it allows one to vary the model used which is what the research used. Further, domain based DFN generation is supported allowing

the simulation of complex 3D DFN. The researcher used persistent radii and enforced negative exponential spacing with single discontinuity per position.

3.3.2 Fracture Orientation

ISRM (1981) described fracture orientation as the attitude of a discontinuity in space. This attitude can be represented by the measured dip and dip direction or dip and strike. Fracture orientations used in this research have been sampled from rock faces through the use of laser data collection techniques. Other reliable sources of fracture orientation include photogrammetry, direct core logging and televiewer (Elmo, *et al.*, 2015).

According to Elmo, *et al.* (2015), aggregate or disaggregate statistical approaches can be utilised to generate DFN models of fracture orientation. In the disaggregate statistical approach which will be used in this research, the user generates individual models per fracture set. The generated statistical model can be represented through any distribution including Fisher, Bingham bivariate Fisher and bivariate Bingham. Of these, the Fisher distribution is most commonly used because it is the "*analog of the normal distribution for fracture data, and because of the ease to derive parameters from field data*," (Staub, *et al*., 2002).

One other distribution for the representation of fracture geometry is the bootstrap distribution. However, this distribution is only applicable if the orientation data is highly dispersed making it hard to define fracture sets. For this research, the disaggregate approach with a normal distribution was utilised (mean and standard deviation were used to populate the model). The disaggregate approach was selected for the research because it allows for more details as individual models are generated per fracture set.

3.3.3 Fracture Terminations

There is a direct correlation between fracture connectivity and fracture terminations which is important in the understanding of rock mass behaviour (Miyoshi, *et al.*, 2017). X-type and T-type terminations shown in Figure 5 are the most encountered fracture terminations.

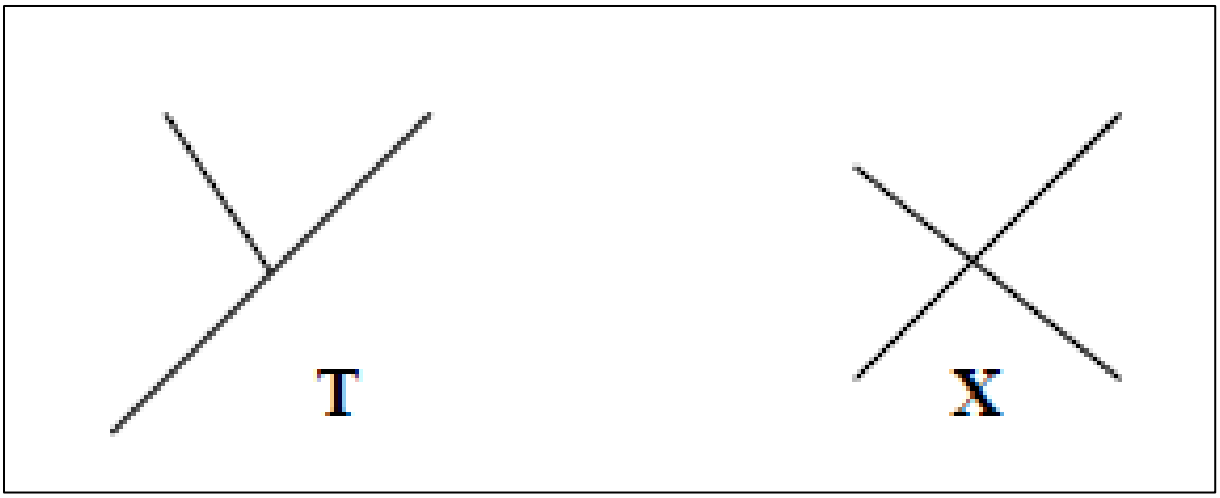


Figure 5: T-type and X-type termination (adapted from Elmo, *et al.* 2014)

T-type terminations represent the order in which fracture sets occurred in nature (e.g. stratigraphic unit with cross-beds joints) Elmo, *et al.* (2014). For this research project, based on structural mapping from the study area, X-type terminations have been assumed because all fracture sets cross one another making it impossible to determine their depositional sequence. However, all sets terminate against prescribed domains (an assumed fault area) indicating that the faults are younger than the fracture sets, hence the faults truncates all fracture sets.

3.3.4 Fracture Length Distribution

The fracture length distribution is defined by ISRM (1981) as the trace length of a discontinuity as observed during mapping. Elmo, *et al.* (2015) cautioned that for DFN modelling, it is critical to differentiate between fracture length (as mapped from rock faces) and fracture radius (radius of a circle equivalent to a polygonal fracture). As previously discussed, the research assumed full persistence over the research area as observed during mapping data.

3.3.5 Fracture Size/Radius

Fracture size is defined as an equivalent radius if the fracture under investigation is assumed to be circular (Miyoshi, *et al.,* 2017). The fracture size information can be acquired from rock faces through cross-examination during site investigation or mapping (Jambayev, 2013). The acquired data can provide a general idea of the length of the fractures. However, the fracture size of a rock cannot be measured directly from boreholes as most of the fracture are very much larger than the drillhole cross-section (Pointe, et al. 1993). For instance, in hundreds of observed core fractures, only a few do not completely cut through the drilled core.

The research assumed full persistence over the research area as observed during mapping data. Therefore, there was no requirement for this project to infer fracture size from fracture traces.

3.3.6 Fracture Intensity

Fracture intensity has been defined by Dershowitz and Herda (1992) as '*the surface area of discontinuities per unit volume*.' Both the size distribution and the number of discontinuities are required for calculating the fracture intensity. Fracture intensity is referred to as P_{ij} intensity, where the subscript *i* refers to the dimensions of the sample, and subscript *j* refers to the dimensions of measurement. The fracture frequency cannot be collected from the currently available sources of data for DFN modelling.

For SiroModel, fracture intensity is an output derived from fracture properties. It combines how often a fracture occur (fracture frequency) and how big the fracture is (fracture size). It is a measure that can be used to assess rock quality and fragmentation for both geotechnical and hydrogeological applications. Investigation of fracture intensity is not part of the objectives of the current research, therefore it was not analysed.

3.4 SiroModel Software

A number of DFN modelling codes are currently available. Almost all of the available computer modelling codes have been proven through peer and industry review to be fit for purpose. Some of the DFN modelling codes are FracMan, FracSim and SiroModel. The research has utilised SiroModel for analysis in this project.

The Open Pit Simulator (OPS), also known as SiroModel, was developed by CSIRO for the Large Open Pit Mine Slope Stability Project of which Debswana is a sponsor and has subsequently undergone many enhancements. The SiroModel application allows the user to create a structural model of a section of an open pit excavation. It also includes a multi-function discrete fracture network (DFN) generator. This allows deterministic discontinuities such as bedding planes and faults and daylighting or confirmed joints (called deterministic joints) to be added to this model. Random joints (called stochastic joints) can be generated upon each simulation based on the statistical parameters for each joint set (Elmouttie, *et al*., 2010)

Termination settings can be used to control the way various discontinuity sets terminate against each other. The software will determine the intersections of all these structures and the presence of all complete blocks within the model, known as a block model. Statistics on each block can be calculated and the blocks can be viewed individually or as an ensemble. Rigid block limit equilibrium stability analyses can also be performed. For confidence in interpreting results from simulations using stochastic joints, a batch of simulations can be run constituting a Monte Carlo analysis. The aforementioned analysis tools can then be used on this batch of simulations. The SiroModel software supports the Baecher model and its variants. The fundamental assumption of the Baecher model is that fractures have either circular or elliptical shapes (Dershowitz & Einstein, 1988).

The software has a DFN generator to provide a practical simulation of rock mass heterogeneity, and polyhedral modelling techniques to model parts of an open pit excavation for slope stability analyses (Adhikary, *et al*., 2016). The DFN generator embedded in SiroModel works based on the availability of information regarding the spatial distribution of the joint sets during mapping. This information includes the dip angle, the dip direction, fracture orientation, thickness, and fracture

size. According to Elmouttie & Karekal (2017), this information is highly significant in predicting the occurrence of daylighting wedges or block stability of the highwall.

SiroModel can create many realisations/simulations of DFNs by utilising the Monte Carlo simulation. This simulation provides the basis for statistical analysis that can be utilised in making informed decisions during mining implementations. Some of the output models/graphs that the research utilised (and will be presented in the results chapter) are hazard map, block location, block volume, back break and bench retention.

The SiroModel software has a limitation in that it cannot detect flexural toppling This limitation does not have any impact on the current research area since the major failure mode is wedge failure.

3.5 SiroModel DFN Application to Open Pit Mines

SiroModel generated DFN modelling is not yet extensively used in rockfall analysis of open pit mines. However, Thoeni, *et al*., (2011) have used DFN modelling for rockfall analysis in open pit coal mining. The authors utilised SiroModel to identify complex polyhedra (rock blocks) and thereby achieve an estimated unstable block size distribution. The unstable block distribution was then utilised in association with site-specific constants to predict rockfall trajectories and velocities. This enabled the open pit coal miner to better assess and quantify the residual risk and required mitigation.

3.6 Chapter Summary

The reviewed literature gives the reader summary of the overview of DFN modelling, DFN model input considerations and requirements. This chapter also provides a brief overview of SiroModel, the selected software for the DFN building in the research area. The SiroModel overview is not designed to be a complete reference in the use of the software package. Available sources and formal training on the use of the SiroModel software is referenced. The literature review chapter also provides a practical case of SiroModel built DFN applications in an open pit coal mine. It is worth noting that there are not many cases that have been found on this regard. This is partly

attributed to the fact that SiroModel is not yet available as a commercial software. As thus the software is only available to its sponsors such as Debswana, De Beers and Anglo American.

4 RESEARCH METHODOLOGY

This research investigates the potential optimisation of bench width by quantifying the Jwaneng site-specific rockfall distributions.

The following methodology was observed when conducting the project:

- Laser scanning mapping of the research area to collect relevant fracture properties;
- Analysis and validation of collected mapping data;
- Modelling of the fracture data using the SiroModel DFN modelling software; and
- Model interpretation, conclusions and recommendations for guidance in decision making.

4.1 Selection of a Research Area

The research area shown in Figure 6 is the Jwaneng Mine Cut 7 western walls.

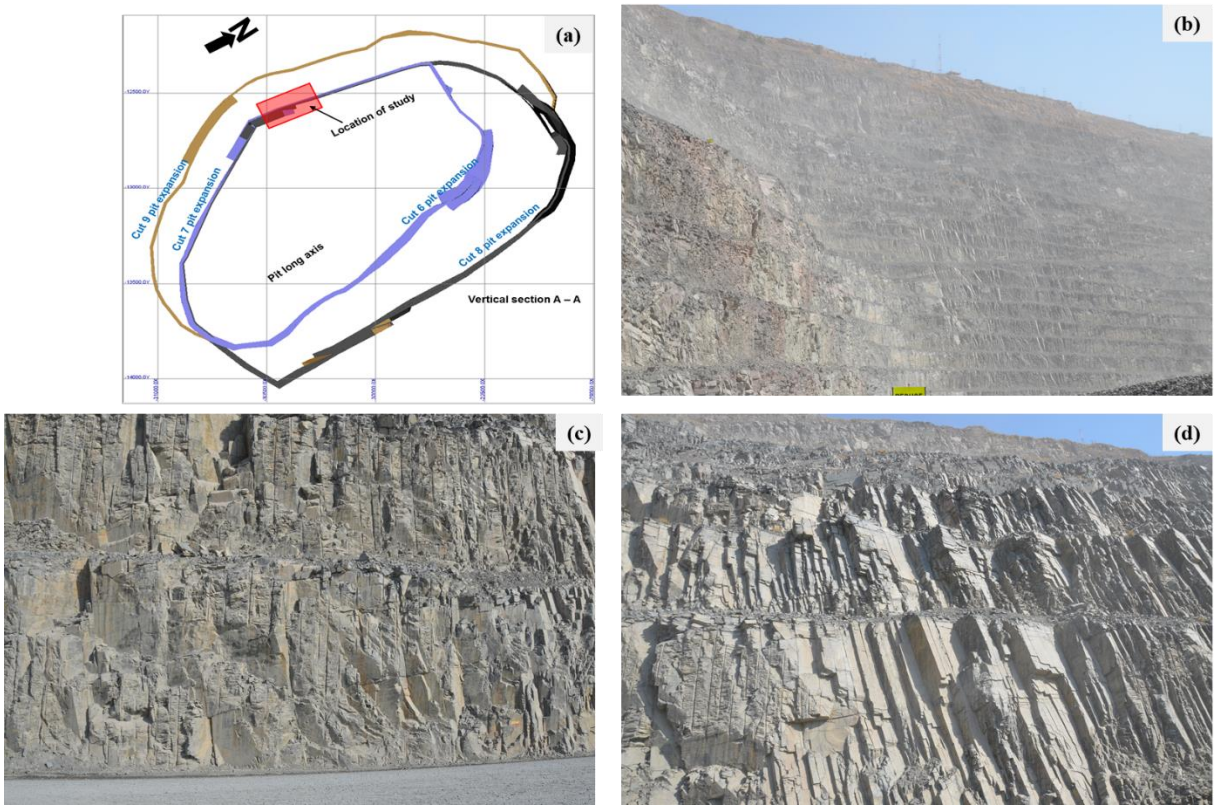


Figure 6: Research area (a) Location of research area within the Jwaneng open pit (b) Overview/large scale view of Cut 7 walls study area (c) & (d) Close-up view of typical fracture orientations/interactions within the Cut 7 research area

There is an elevated risk of rockfalls on these walls when compared to the rest of the open pit. This area was selected for the research because it offers the research and the mine an opportunity to optimise bench width designs through the investigation of rockfall distribution. The selected portion of the Cut 7 walls offers a good representation of fracturing/jointing on the western walls. Investigation of Cut 7 walls also provides an opportunity to optimise the newly started Cut 9 pushback. The Cut 9 pushback is the open pit expansion currently being implemented directly behind the Cut 7 walls. Applicability of results from the Cut 7 research is possible because various data collection and analysis regimes undertaken in the mine have proven geological (lithology and structure) persistence.

4.2 Data Collection and Manipulation

DFN data can be collected from good quality-oriented core samples. The data can also be collected by utilising, either conventional or digital mapping techniques. For this research, laser scanning mapping (which is a type of digital mapping technique) has been used for data collection.

The laser scanning mapping technique has been a favoured instrument for use in this project because it allows for remote mapping thereby keeping personnel from the elevated rockfall risks under the open pit high-walls. Other advantages of laser scanning mapping include its speed, high data density, accuracy and precision in terms of measurement.

4.2.1 Laser Scanning – Survey Positioning

Jwaneng mine surveyors have outlined a thorough process to ensure that data collected in the open pit satisfies industry acceptable accuracy in terms of geospatial referencing and location. To achieve this, the Jwaneng Mine Survey Control Network is utilised. A Survey Control Network is a group of survey beacons interconnected in relation to their geospatial position, as shown in Figure 7 (not to scale).

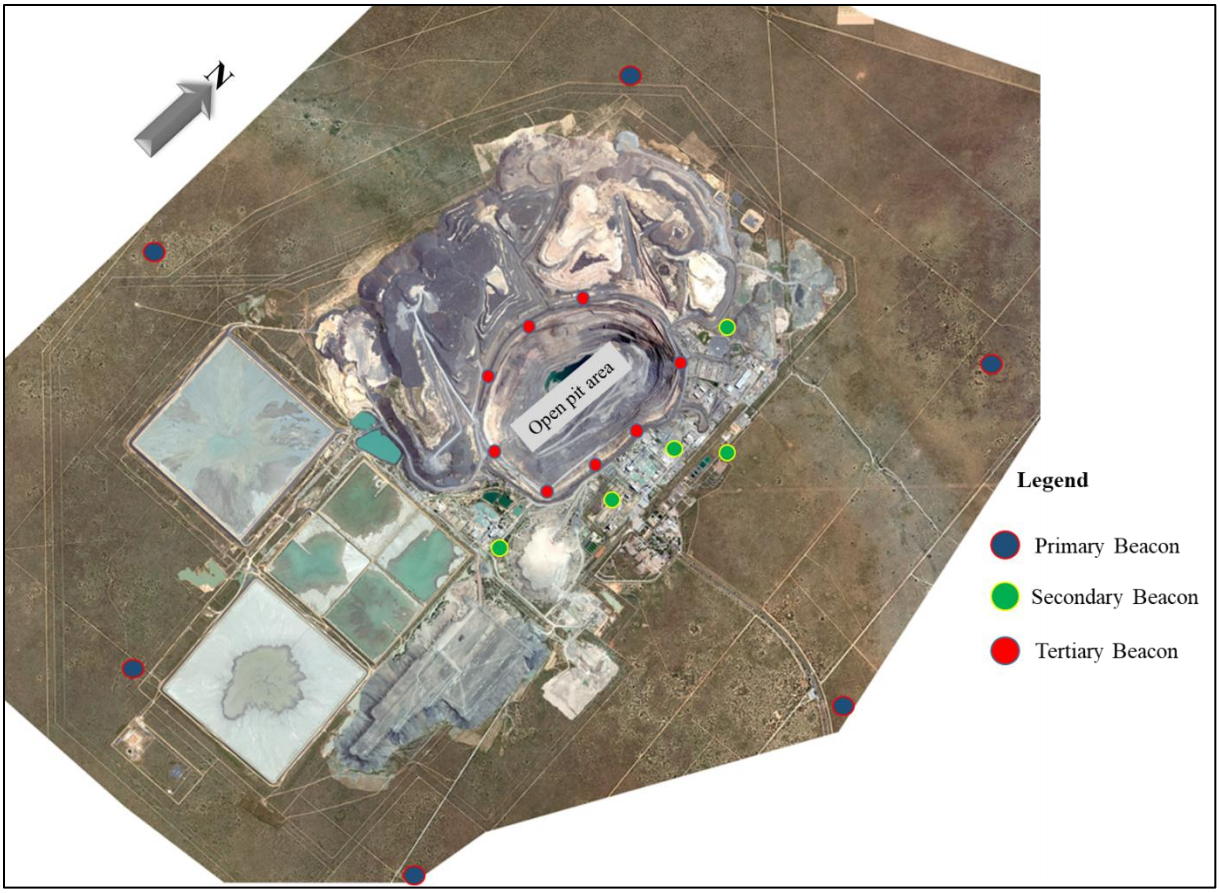


Figure 7: Jwaneng Mine Survey Control Network

In Jwaneng Mine, a survey beacon is constructed by drilling through the Kalahari sand to hard rock. A reinforced concrete pile is then constructed into the hole protruding the ground level by at least 1.5 m. Piling is done to ensure that there is no horizontal or vertical movement after concrete settlement resulting in an unstable beacon. A survey beacon constructed as per Jwaneng Mine standard is shown in Figure 8.



Figure 8: Jwaneng Mine Survey Beacon

Jwaneng Mine beacons within the Survey Control Network are categorised into three types based on the proximity to the pit and therefore inherent long term stability of the beacon;

1. Tertiary beacons are located in the open pit where there are mining activities such as drilling, blasting and movement of heavy machinery. These beacons are used for survey measurements and geo-referencing in the open pit. The accuracy of these beacons maybe compromised by mining activities. Survey integrity checks are conducted on these beacons daily before use.
2. Secondary beacons are located outside the mining area but within 3 km of the open pit relaxation zone. Survey integrity checks are also performed on these beacons before they are used for any survey measurements to ensure that they are within tolerable error limits.

3. Primary beacons are placed at distances greater than 3 km of the open pit relaxation zone, on ground that is assumed to be continually stable. Survey integrity checks are done on these beacons once a year to ensure that they are within tolerable error limits.

Survey integrity checks are done on the entire survey control network to the same survey accuracy through static GNSS observations method followed by the post-processing of raw GNSS data for horizontal control. The vertical control survey checks are done through precise levelling. The post-processing and levelling results are sent to the Department of Surveys and Mapping at the Director General's Office for approval and filing.

4.2.2 Laser Scanning – Data Collection

A 100 m long face was scanned using the Maptek I-Site 8820 Laser Scanner shown in Figure 9. According to Maptek (2019), the vendor of the laser scanner, the I-Site 8820 laser scanner has a 5 mm range accuracy and 4 mm repeatability at a range of 100 m.



Figure 9: The Maptek I-Site 8820 Laser Scanner

The laser scanner itself does not have any on-board GNSS facility. So, to localise the point cloud coordinates to the open pit, georeferencing is conducted (also known as laser scanner registration) to convert the laser scanner coordinate system to the local coordinate system.

This registration is done by the use of two survey control points:

1. The first being the laser scanner's occupation point, which is observed by a roving GNSS receiver placed on top of the scanner to measure the laser scanner's location. A survey check is performed on the roving GNSS receiver before this exercise using the survey control network.
2. The second is the sighting to backsight or reference station. This is done by rotating the laser scanner about its occupation point and bisecting the reference station using the telescope and crosshairs in the laser scanner. A survey accuracy check is performed on the roving GNSS receiver prior to this exercise using at least two secondary beacons, including the one to be used as a backsight.

Comparison of outputs of these two (2) georeferencing methodologies is used to register the laser scan and localise the point cloud to the mine grid.

The laser scanning of the Cut 7 walls was undertaken at the 40 m range (from the highwall). A total of three set-ups were undertaken along the 100m long face and stitched together to form a point cloud. Through the use of mathematical ratios on range versus face length, the point density was calculated to be 1.6mm for the research area. The research area had a 40 m range and three setups along a 100 m long face. The image produced and used for this project is shown in Figure 10.

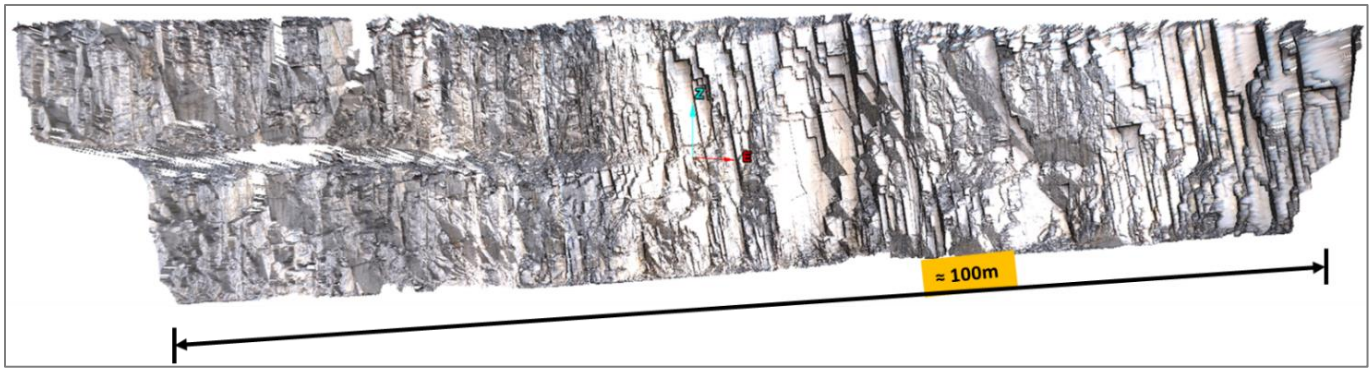


Figure 10: Cut 7 wall image produced from Maptek Maptek I-Site 8820

4.2.3 Maptek PointStudio 8 Structural Mapping

Mapping was conducted on the Maptek PointStudio 8 software that is provided by Maptek for manipulation of data collected using their laser scanners. This software provides various options for mapping geological structures. For this research, the 'extract discontinuities' tool was used. This is a semi-automatic option of mapping structures from a laser scanner generated image. The 'extract discontinuities' tool does the automatic mapping of fracture sets but prompts the user to guide it to provide inputs as shown in Figure 11. This figure represents the use-defined settings that were applied for the mapping of the Cut 7 walls for the current project.

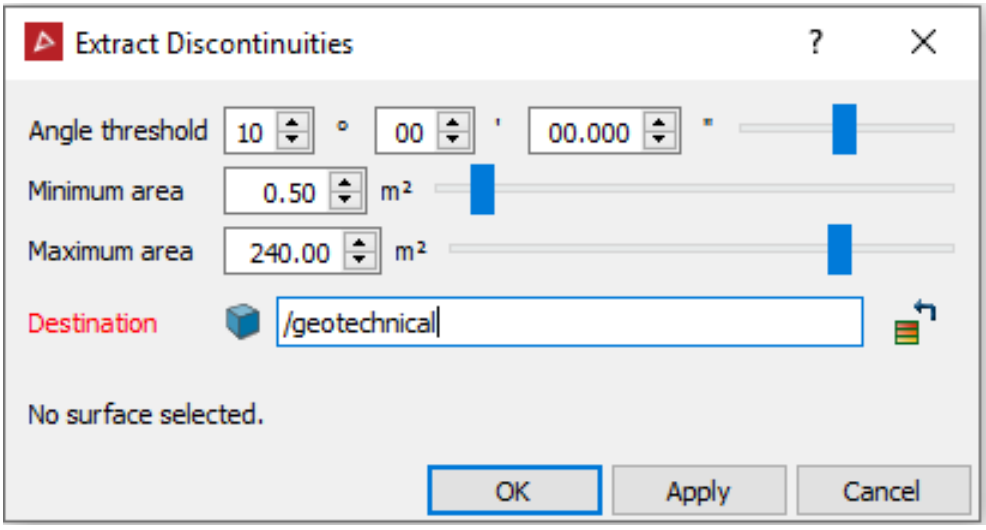


Figure 11: The settings on the automatic mapping tool

In Figure 11, the angle threshold refers to the maximum angular difference for two structures to be defined as part of the same set. This entity considers both the dip and dip direction of a fracture/joint. The selected angle threshold is acceptable industry standard. The ‘minimum area’ and ‘maximum area’ are the areal limits of detection of fractures that should be detected and mapped. The selection of the limit of detection areas is based on historic observations of rockfalls in the Jwaneng open pit.

Literature has shown that using automatic detection tools may result in over-segmentation of fractures. Over-segmentation results in the under-estimation of structure sizes and over-estimation of structure numbers. The user-defined settings of extents of areas of detection assist in ensuring that over-segmentation does not occur.

Using the parameters discussed above, the Cut 7 wall was mapped and the fracture sets detected are shown in Figure 12(a). Four (4) Fracture Sets were mapped within the Cut 7 walls research area. The Fractures are coloured as per the legend on the diagram. This colour scheme will be maintained throughout this research report.

For Fracture Set 4, the minimum area of detection has been reduced to $0.1m^2$. This reduction in size was deemed necessary for a fair sampling of Fracture set 4 considering its poor exposure. The poor exposure of this set is because it dips away from the pit and therefore its ‘hidden’ from view. Figure 12(b) shows mapped fractures when the area of extent is unconstrained. There is over-sampling of fractures when the mapping is unconstrained.

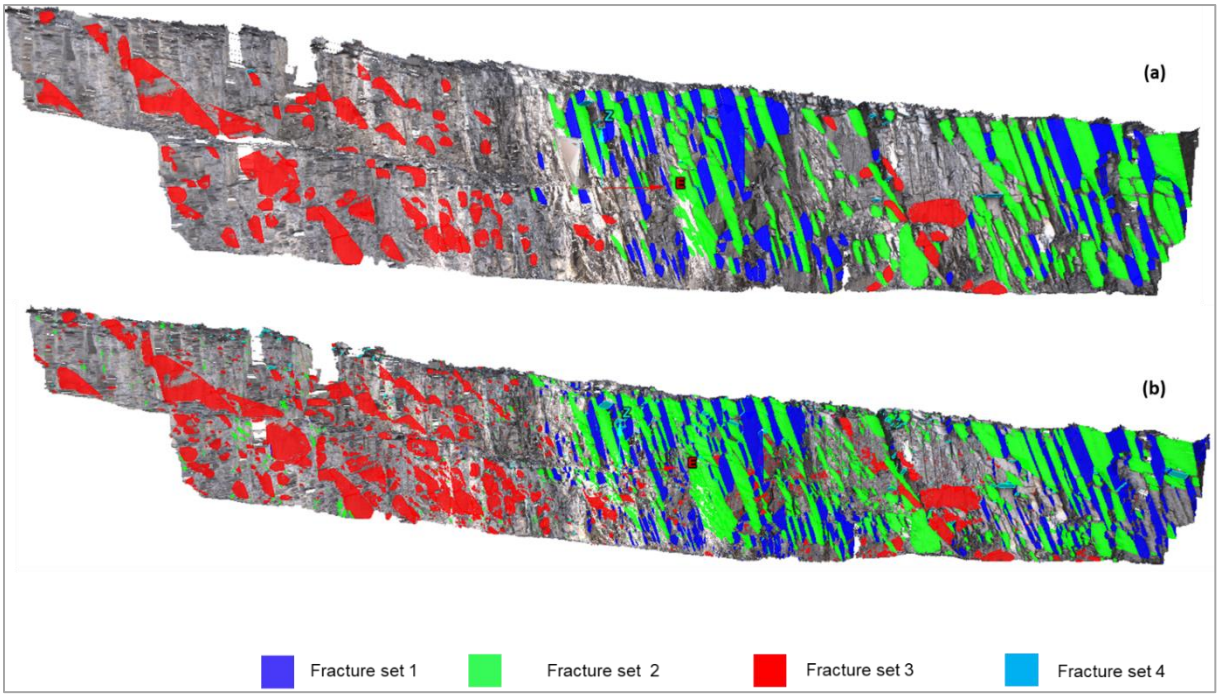


Figure 12: Cut 7 wall mapped fracture sets – (7a) is the mapping with user defined limits on area of extents (7b) shows fractures where limits were not defined, the system minimum and maximum areas of extents were used

4.3 Analysis of Fracture Sets Attributes

The mapped fracture sets attributes are presented in the following figures. These Figures represent the 'unweighted' data from the area of study and are discussed in the following sections.

4.3.1 Fracture Orientation

Figure 13 shows the planes and poles of the fracture sets identified within the study area. There are four (4) fracture sets within the Cut 7 walls research area. Fracture Set 4 is synonymous with the bedding within the Jwaneng open pit.

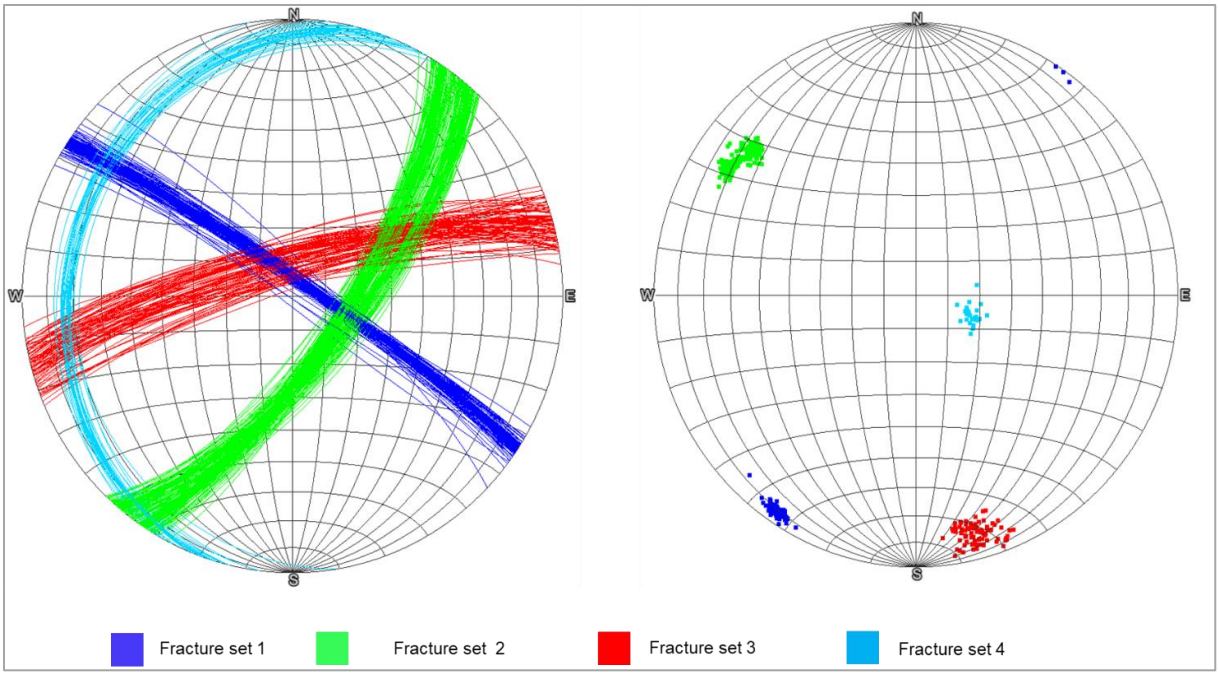


Figure 13: Stereographic plot of mapped Fracture Sets (planes and poles)

4.3.2 Fracture Spacing

The fracture spacing, represented in Figure 14 approximate a negative exponential distribution for Fracture Sets 1, 2 and 3. Fracture Set 4 is approximately a binomial distribution.

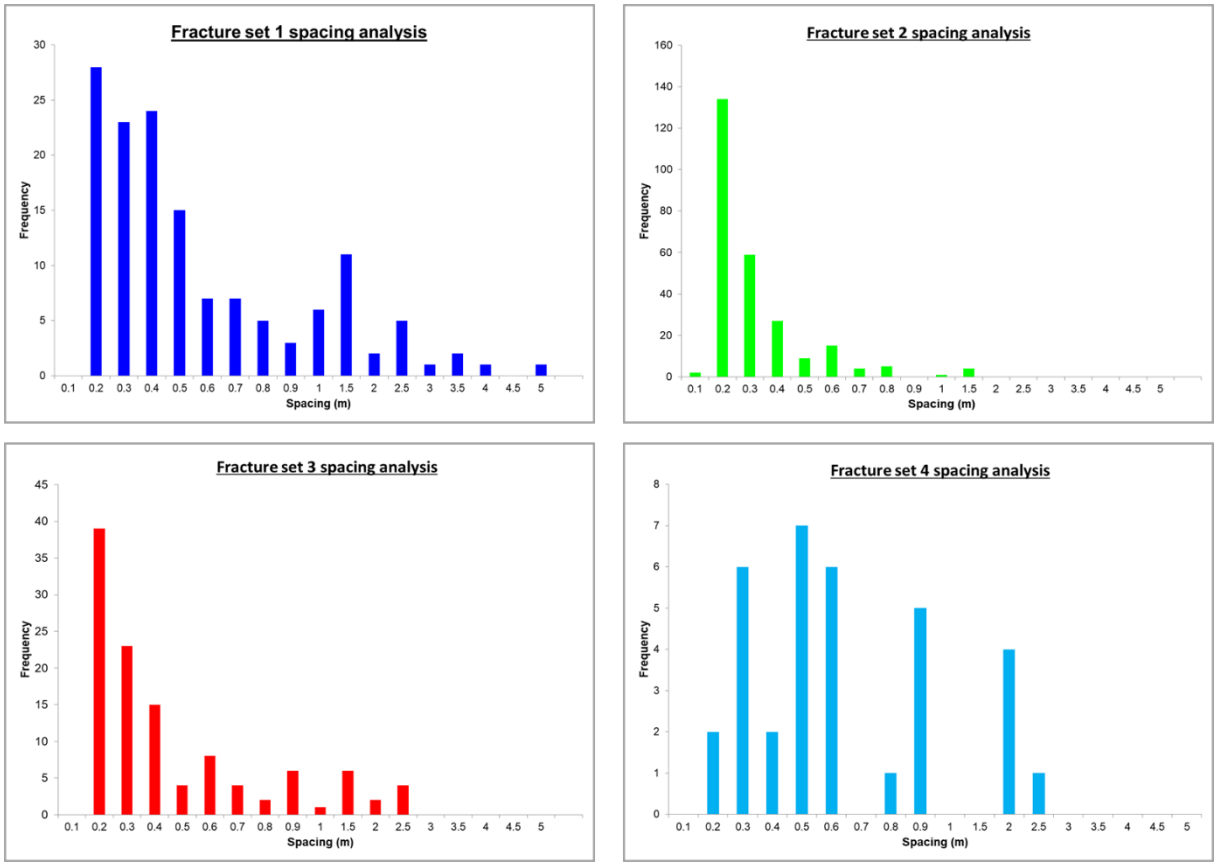


Figure 14: Fracture spacing distribution per Fracture Set

4.3.3 Fracture Length Distribution

The fracture length distribution of all the four mapped fracture sets approximates a negative exponential distribution. Given the sampling bias introduced by the automatic detection of fractures versus the observation and analysis of the research, domain bound persistent structures were deemed to be an appropriate representation. Thus, the fracture length distributions presented in Figure 15 were not utilised for this research.

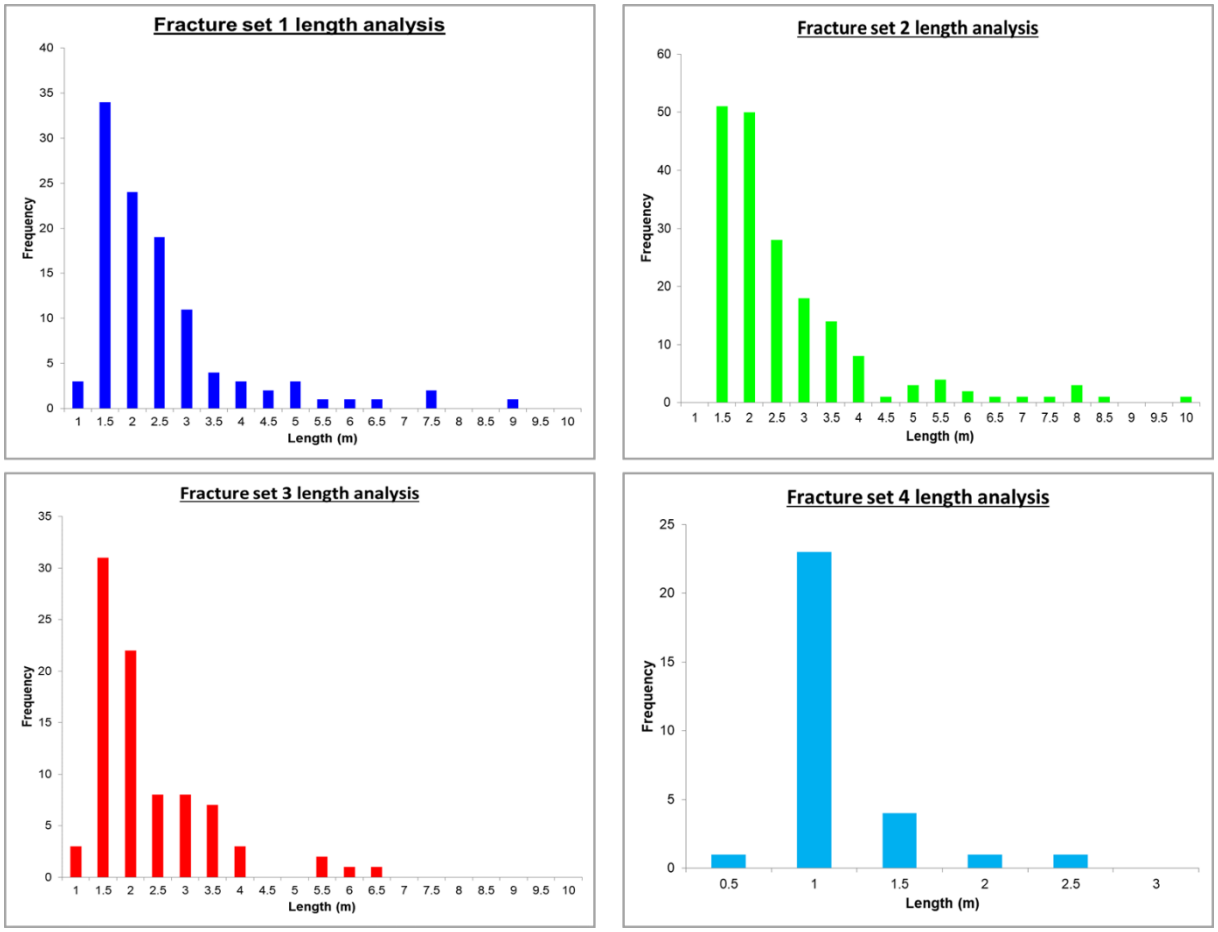


Figure 15: Fracture length distribution per set

4.3.4 Fracture Terminations

As discussed in the literature review, fracture terminations may be difficult to record because both X and T terminations may co-exist. However, for this research, X terminations were assumed for the Cut 7 research area.

4.3.5 Kinematic Analysis

Kinematic analysis assess possible bench scale failure through the various failure mechanisms; planar, wedge and toppling failure modes. The failure mechanism is defined by the interaction of Fracture Sets with the open pit geometry. The Jwaneng open pit research area geometry measured and used was dip/dip direction of 90°/155°. Kinematic analysis of the unweighted data. Table 5

summarizes the failure percentages per failure mode on the research area. These failure modes are discussed in detail in sections 4.3.6 to 4.3.8.

Table 5: Summary of failure percentage per failure mode on the study area

Failure mode	Total number of poles / intersection	Critical poles / intersections	Failure percentage (%)
Planar failure	417	23	5.51
Wedge failure	85078	38502	45.26
Direct toppling	417	0	0
Flexural toppling	417	88	21

4.3.6 Planar Failure

Authors including Wyllie & Mah (2004) provide the geometry of a possible planar failure such as that shown in Figure 16.

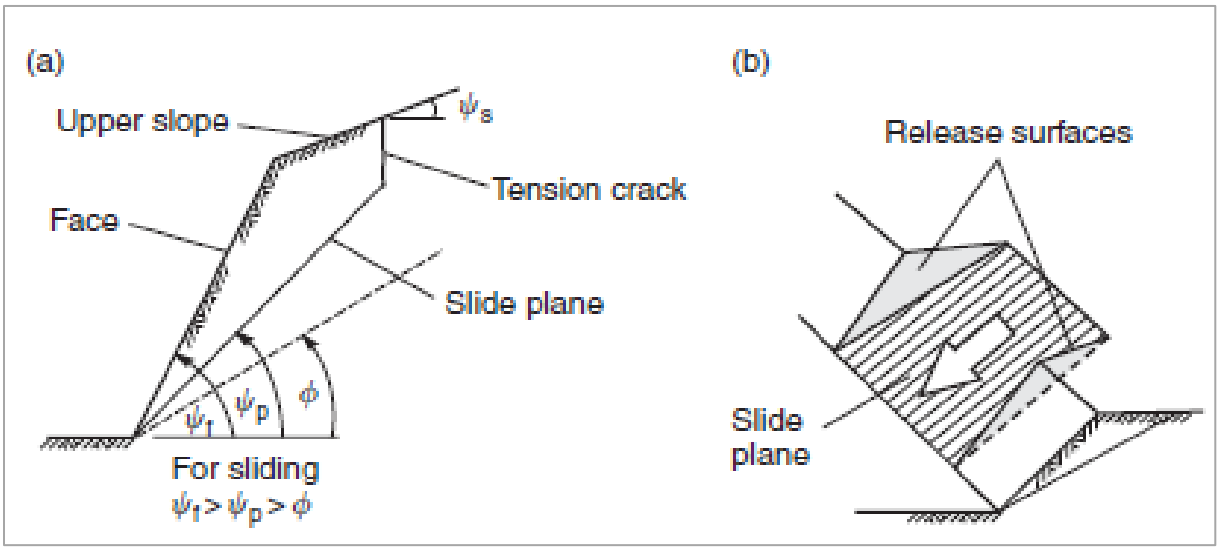


Figure 16: Geometry of plane slope failure: (a) Typical view of a plane failure; (b) release surfaces at the ends of the plane failure (Wyllie & Mah, 2004)

A planar failure is most likely to occur when the sliding plane strikes parallel to the slope face (within ±20°). This sliding plane must have a dip that is less than the slope face but greater than

the slope friction angle. A dip angle less than that of the slope face allows the sliding plane to 'daylight' in the slope face. According to Wyllie & Mah (2004), the upper end of the sliding plane must either intersect the upper slope or terminate in a tension crack to create an initiation point of failure. "*Release surfaces that provide negligible resistance to sliding must be present in the rock mass to define the lateral boundaries of the slide*" (Wyllie & Mah, 2004).

The research used the above guidelines by Wyllie & Mah (2004) and a stereonet to assess the possibility of planar sliding on the study area. The results of the assessment are shown in Figure 17(a). Figure 17(a) suggests that there is no planar failure in the area of study. A keen Geotechnical engineering experience, outlook and analysis becomes vital to realise that the green poles (Fracture Set 2) lies just outside the set lateral limits. Figure 17(b) shows increasing the lateral limits slightly, by 4°, planar failure is predicted to occur in Fracture Set 2.

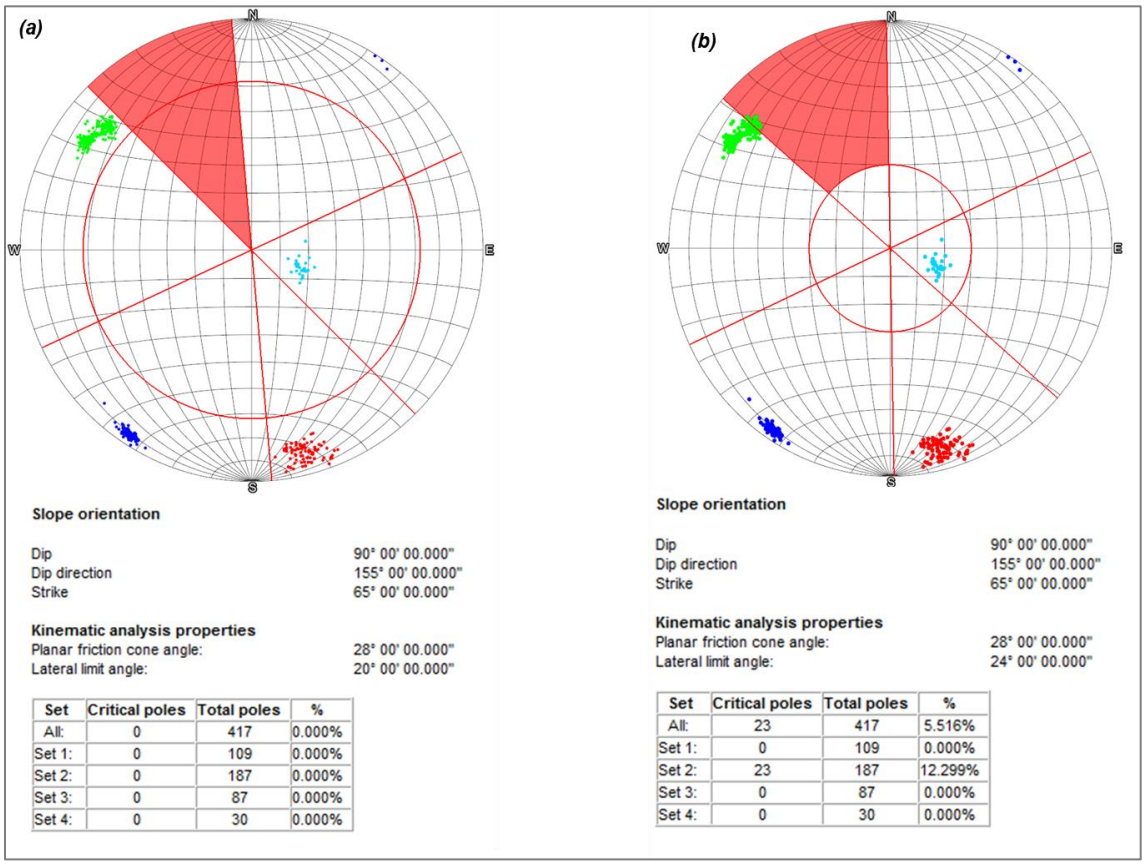


Figure 17: Cut 7 walls Planar failure analysis stereographic projection from Maptek I-site software

4.3.7 Wedge Failure

Wedge failure occurs when rockmass slides along the intersection of two planes. Figure 18 adapted from Rajesh (2014) shows the geometrical conditions that must be satisfied for a wedge failure to occur.

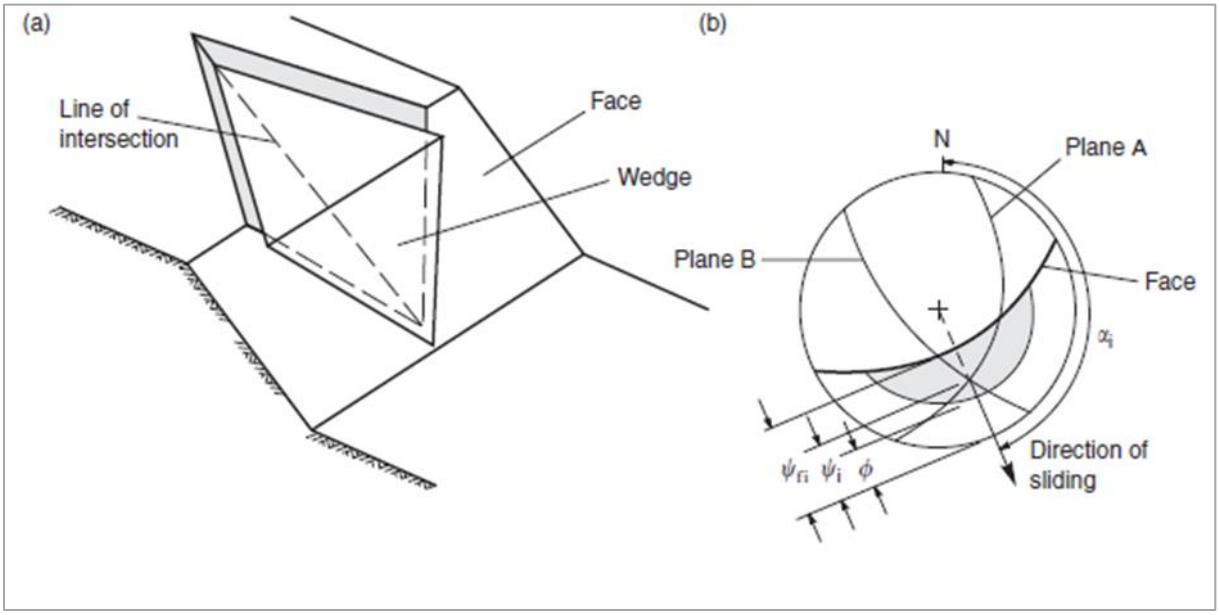


Figure 18: Geometry of wedge slope failure; (a) pictorial view of wedge slope failure; (b) Stereoplot showing the line of intersection (Rajesh, 2014)

Rajesh (2014) outlines the following as critical geometrical conditions for a wedge failure;

- The two planes must intersect behind the slope face and dip out of the wall;
- The line of intersection of the two plane '*daylights*' into the open pit, that is, this line of intersection must have a dip angle that is less than the slope angle; and
- The line of intersection of the two planes must have a dip angle that is greater than the rock friction angle.

Following the guidelines of Rajesh (2014), wedge failure potential was predicted as shown in Figure 19. From this diagram, it can be observed that all of the intersected Fracture Set 4, which has been identified as bedding will fail as wedges.

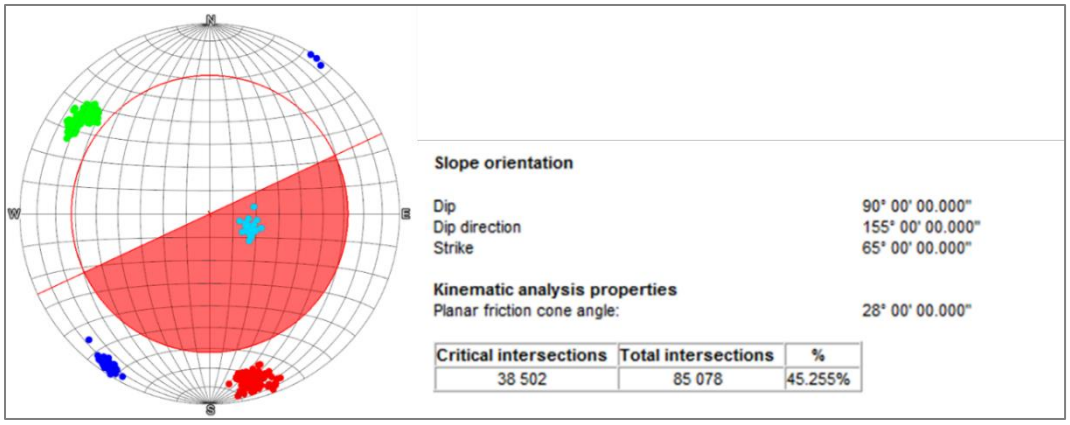


Figure 19: Cut 7 walls wedge failure analysis

4.3.8 Toppling Failure

Toppling failure occurs when rock slabs with steeply dipping joints rotate about a fixed point at the base of the slope resulting in slippage of the rock layers. According to Prajapati (2017), it is essential for the slabs to dip away from the slope for toppling to occur.

Two major types of toppling have been defined in literature. The toppling modes are discussed below and shown in Figure 20.

1. **Direct toppling** – critical overturning moment occurs due to a block centre of gravity that lies outside the base of the block.
2. **Flexural toppling** – '*mode of failure involving the bending of interacting rock columns formed by a single set of steeply dipping discontinuities, such as regular bedding planes, foliation, or joints*' (Adhikary, *et al*., 1997).

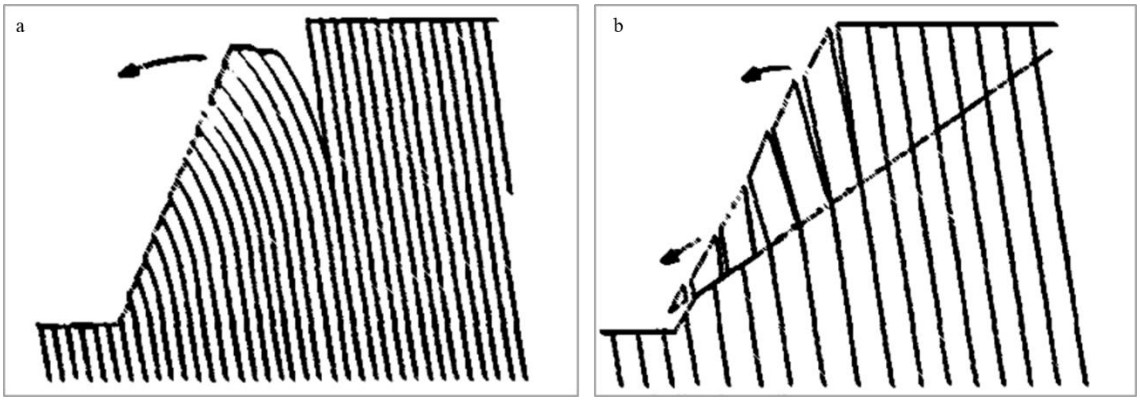


Figure 20: Geometry of toppling failure; (a) Direct toppling along an existing daylighting plane/bedding (b) Flexural toppling mechanism (Adhikary et al. 1997)

Following these definitions, an assessment of the likelihood of toppling on the research area was undertaken. The results of the assessment are shown in Figure 21. The analysis suggests that there is no direct toppling as presented in Figure 21(a). However, all fractures of Set 3, representing 21% of the mapping data, are expected to experience flexural toppling failure as shown in Figure 21(b).

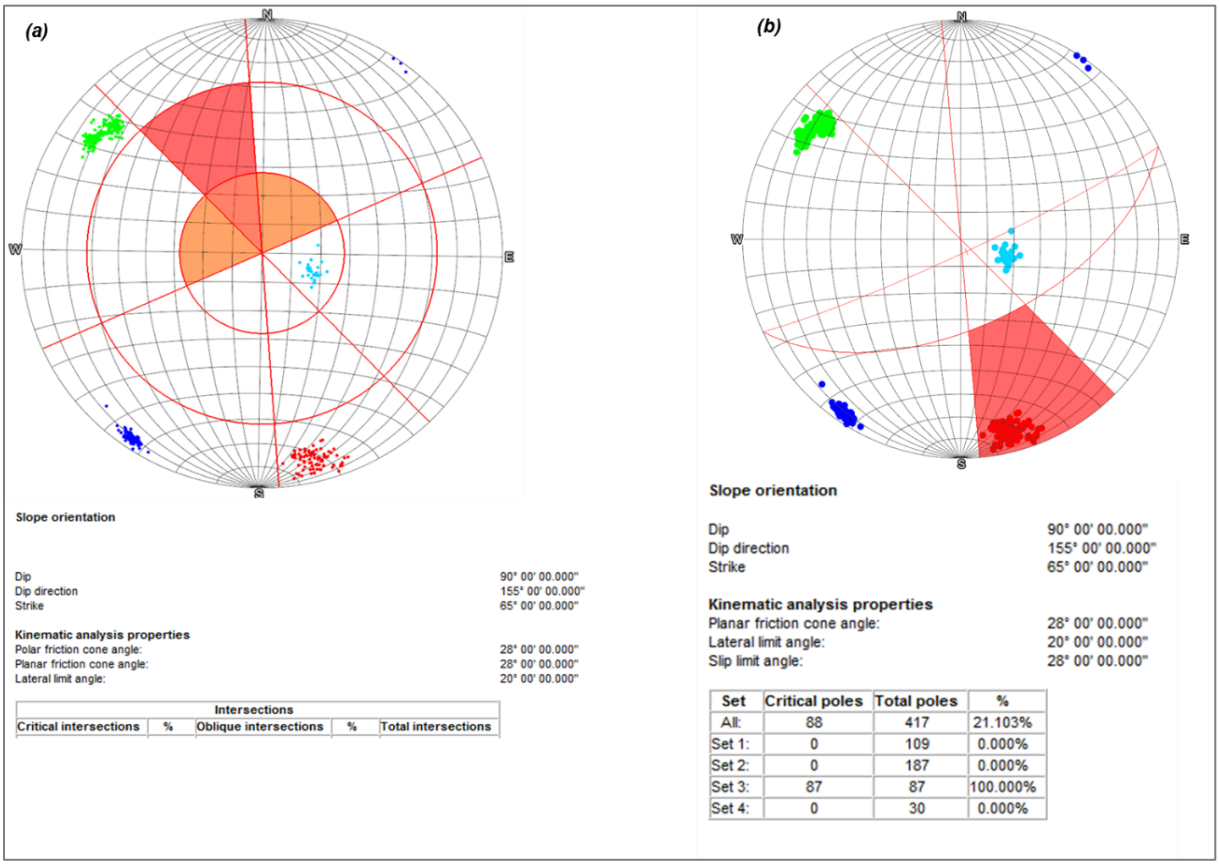


Figure 21: Cut 7 walls toppling failure analysis (a) Flexural toppling (b) Direct toppling

4.4 Chapter Summary

Chapter 4 provides an overview of the data collection techniques that were utilised. The chapter also provides the quality assurance and quality control protocols that were employed to ensure that the data is compliant to set industry standards.

This chapter also provides an analysis of collected data. The analysed data forms an input into the DFN modelling. DFN modelling is the objective of this research project.

5 DFN MODEL BUILDING AND CALIBRATION

A DFN model of the research area was built with open pit geometry properties and rockmass properties as shown in Table 6.

Table 6: Research Area DFN Model inputs

Attribute name	Fracture type	Dip (°)	Standard deviation	Dip direction (°)	Standard deviation	Orthogonal mean trace spacing
Fracture Set 1	Stochastic	85	1.34	33	1	1
Fracture Set 2	Stochastic	72	1.37	126	1	0.7
Fracture Set 3	Stochastic	79	2.15	345	2	0.8
Fracture Set 4	Deterministic	18	0	289	0	NA
Open pit geometry	NA	90	0	155	0	NA
Mapped area	NA	85	0	155	0	NA

Table 6, represents measured and/or mapped data and associated statistical representation used for building the DFN model. The standard deviation represent a very low scatter of the stochastic fracture. The low scatter indicate highly uniform orientation of mapped Fractures; this is a good representation of observations in the field.

For stochastic fracture sets, the following attributes were also utilised as inputs:

- Zone parameter of zero (0);
- Poisson distribution for joint centres;
- Exponential distribution for joint spacing;
- Uniform joint distribution;
- Fully persistent lengths of fractures; and
- Enforced terminations within set domains

For all Fractures Sets, a cohesion of zero (0°) and a friction angle of 36° were used as inputs. Zero (0°) cohesion represents a total loss of cohesion on the analysed ‘near surface’ rocks due to mining activities such as blasting. The friction angle has been determined from laboratory testing.

The success of any model to produce acceptable results is highly attributed to its calibration, that is, the level of the model's success in simulating reality. Successful calibration becomes even more critical for models that are to be used as prediction tools for natural phenomena such as rockfalls which is the subject of this research.

5.1 Calibration of the DFN Model

An extensive process was followed to ensure successful calibration of the created DFN model before any analysis could be run on the model. The following sections presents the process followed to calibrate the DFN model.

5.1.1 Fracture traces Calibration

Figure 22 is a calibration of fracture traces simulated within the SiroModel against observed fractures in the research area.

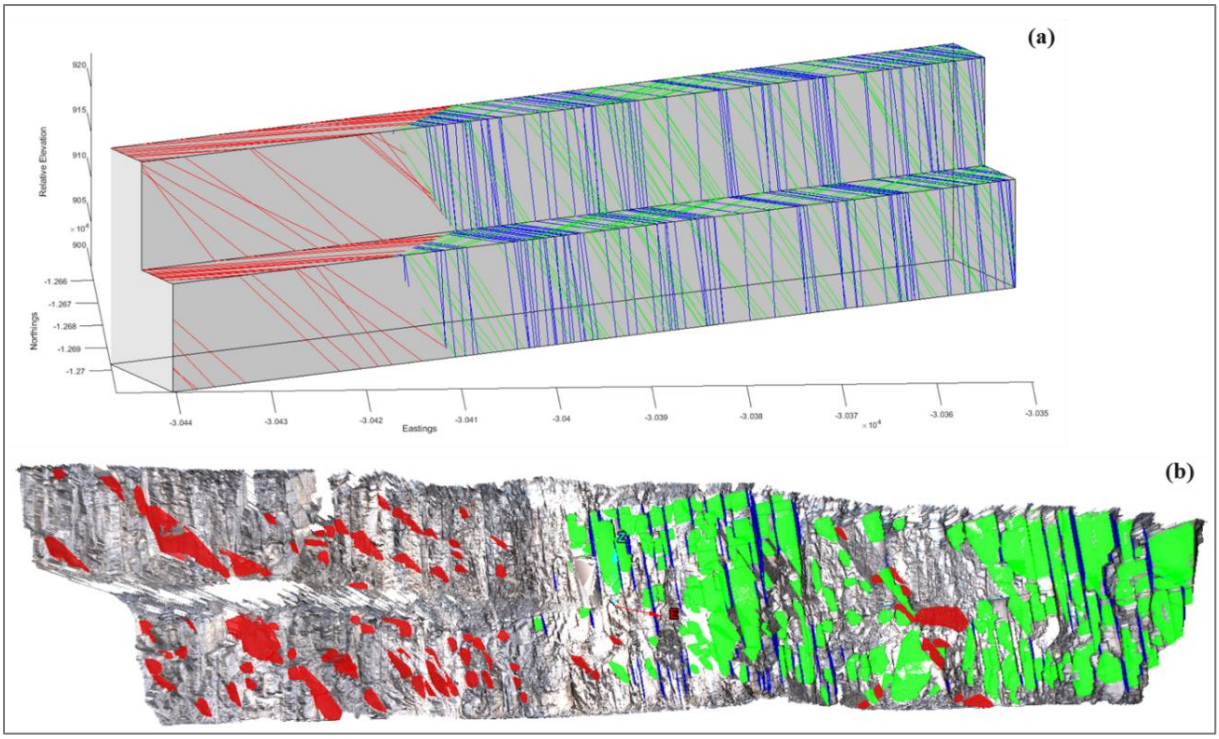


Figure 22: SiroModel fracture traces calibration (a) Simulated fracture traces within SiroModel software (b) mapped fractures on the study area

The simulated traces were achieved by using attributes shown in Table 6 as well as the other fracture distributions discussed in earlier chapters. The distribution of the simulated fracture sets was controlled by the use of termination laws within set domains. There is an observed acceptable correlation between the simulated fracture traces and the mapped fractures; thus, the first step of calibration is deemed to be successful.

5.1.2 Stereoplot Calibration

The next step of the SiroModel calibration is to ensure that the statistical stereoplot data of the simulated model traces correlates well with the mapped data. The stereoplots of the simulated model and mapped data were used for this exercise. As shown in Figure 23, a good correlation exists between these two data sets, further proving the successful calibration of the SiroModel. There is however an under-sampling of Fracture Set 4 observed in the SiroModel simulation. The under-sampling is attributed to the deterministic modelling of this fracture set.

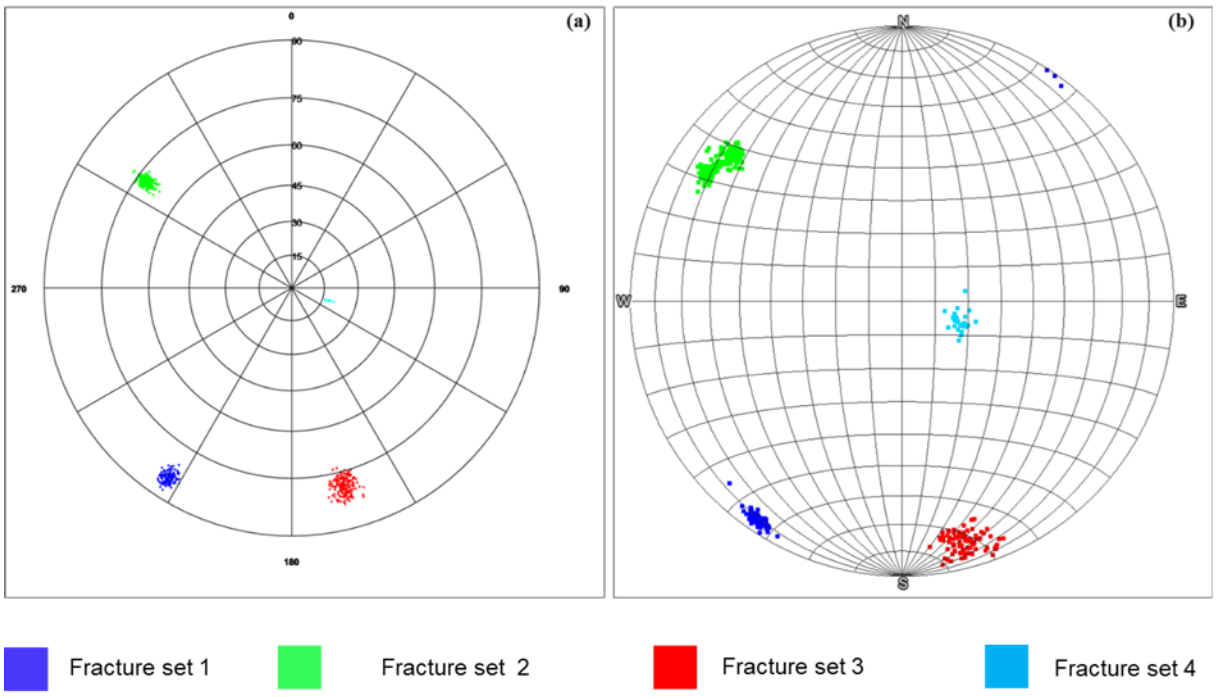


Figure 23: SiroModel stereoplot data calibration (a) Simulated stereoplot data from SiroModel software (b) mapped stereoplot data of fractures on the research area

For a more quantitative comparison, the SiroModel simulated fractures and the mapped fractures were plotted on a single stereoplot shown in Figure 24.

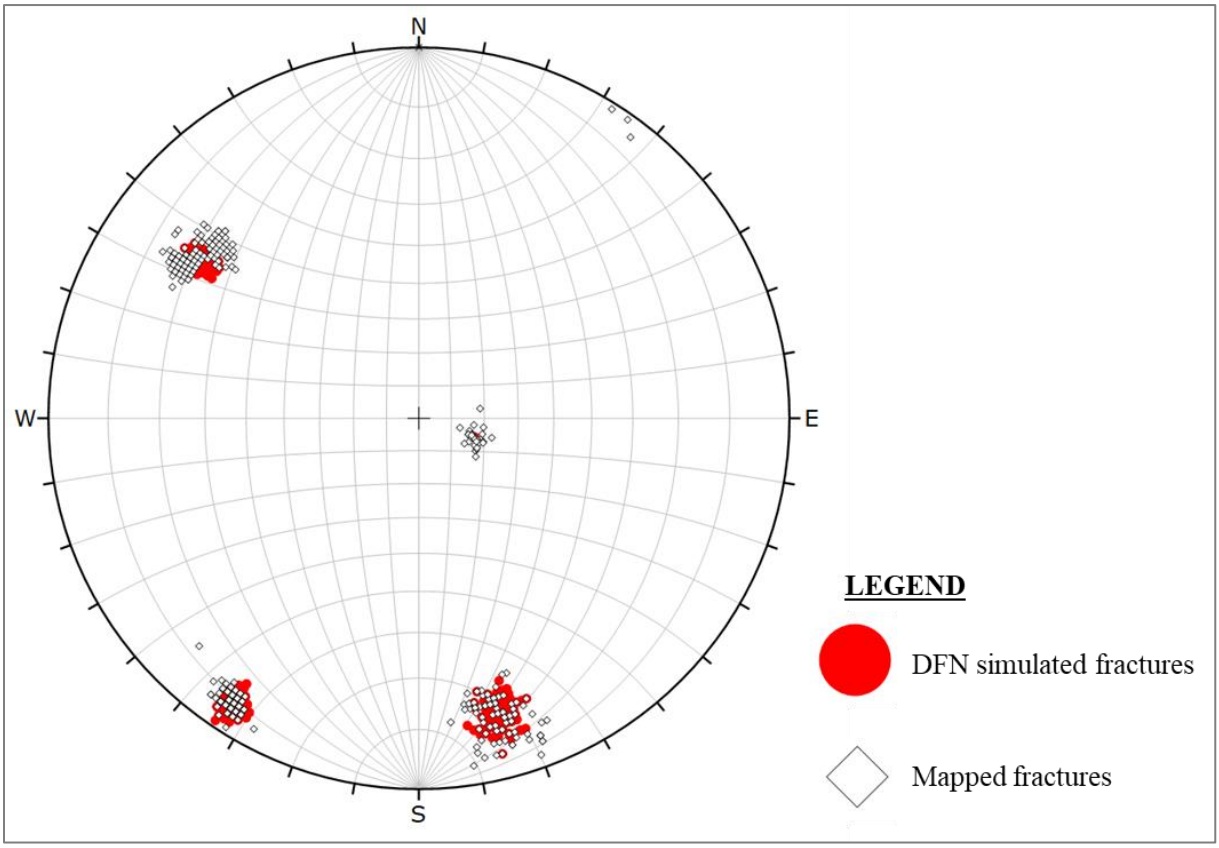
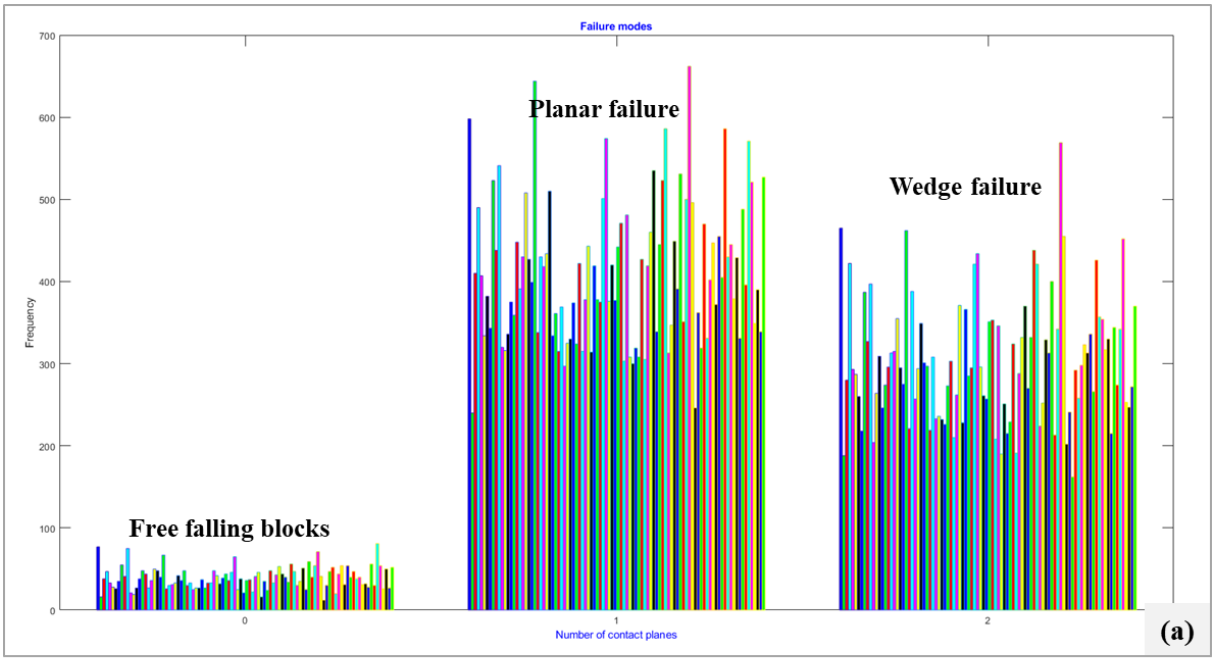


Figure 24: Stereoplot comparison of Simulated fractures and mapped fractures

This figure shows an excellent correlation between the two data sets, further proving that the calibration of the DFN model is successful and as such the model can be used for the analysis of the research area. The under-sampling of Fracture Set 4 as discussed in Figure 23 is still observed.

5.1.3 Kinematic Analysis Calibration

Figure 25 is a calibration of the SiroModel based on the expected failure mechanisms.



Failure mode	Total number of poles / intersection	Critical poles / intersections	Failure percentage (%)
Planar failure	417	23	5.51
Wedge failure	85078	38502	45.26
Direct toppling	417	0	0
Flexural toppling	417	88	21

(b)

Figure 25: SiroModel failure mode calibration (a) Failure modes from SiroModel simulated data (b) Failure modes from mapped data of the research area

By comparing Figure 25(a) and Figure 25(b), the following are observed with regards to the failure modes:

- SiroModel predicts a higher potential frequency of occurrence of planar failure. In this regard, the research has a higher confidence in the SiroModel results. This is because results of kinematic analysis have a higher likelihood to be influenced by user influence decisions. When using stereoplots for kinematic analysis, failure is predicted within limits (lateral limits between the open pit geometry and the fracture orientations) that are user-defined. For example, in this project, it has been shown that setting the lateral limits to 20°

results in no planar failure. Increasing these lateral limits by just 4° shows potential planar failures (see Figure 17).

- There seems to be a visual correlation between the SiroModel predicted failure probability and the wedge failure predicted using mapped data on a stereoplot.
- There is no flexural toppling predicted by the SiroModel simulations in comparison to the mapped data stereoplot. This is a software limitation; SiroModel is not configured to predict flexural toppling. However, toppling is not the major failure mode of concern in the reseaarch area. Therefore, SiroModel is considered to still be a tool that is fit for purpose.
- SiroModel predicts some potential free failing blocks. The stereoplot does not have the capacity to predict free failing blocks as it utilises fracture orientations and their interactions to predict potential failures. The free failing blocks have been observed in the field.

5.2 Chapter Summary

This chapter is a summary of inputs into the SiroModel software. The chapter also discusses the various calibration processes that were undertaken to ensure that the model simulation correctly represents field observations.

It is outside the scope of this project to take the reader through a step-by-step process of model building in SiroModel. For a detailed process on using SiroModel, the reader is directed to CSIRO (2019).

6 RESULTS AND ANALYSIS

Statistically acceptable results are achieved by the utilisation of Monte Carlo simulations on realised blocks (potential rockfalls). The realized blocks were calibrated against field observations before the Monte Carlo computations were undertaken. After numerous trials, the number of Monte Carlo simulations was set to one hundred (100). One hundred simulations have been proven to be a good statistical representation as they fill the histogram as per statistical requirements (see Figure 26).

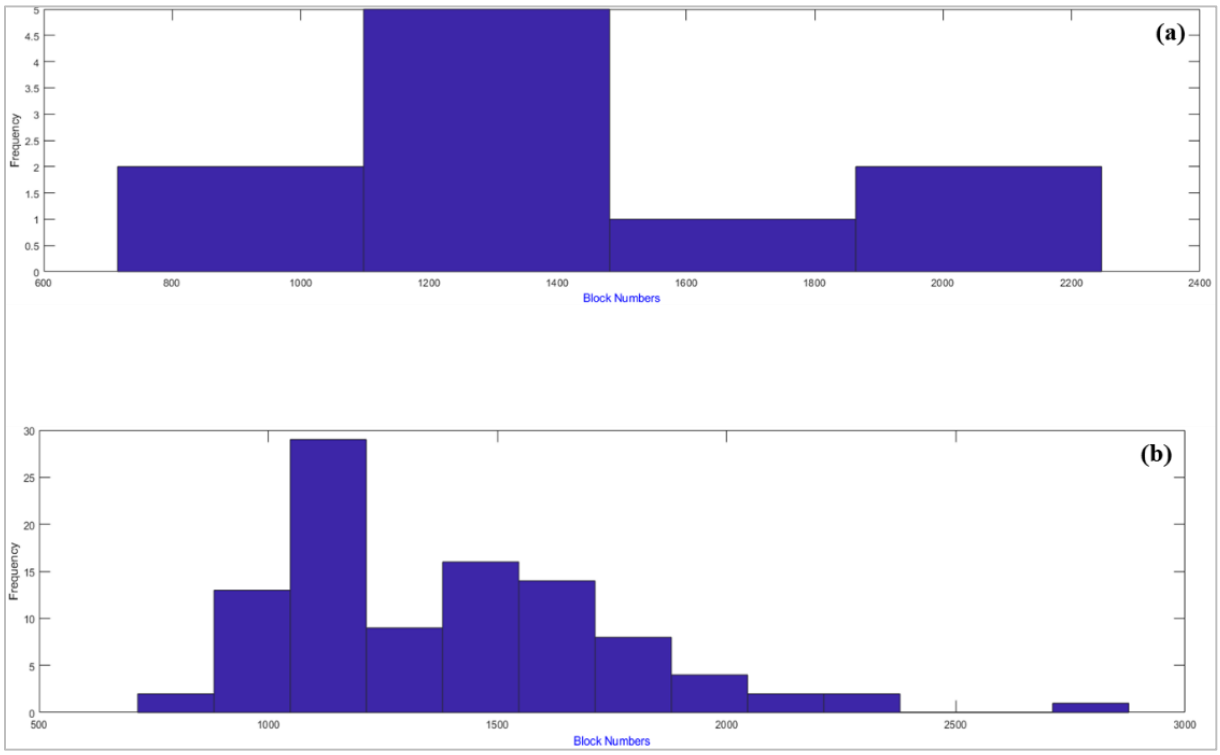


Figure 26: Monte Carlo simulations (a) Ten Monte Carlo simulations (b) One hundred Monte Carlo simulations

Figure 27 shows blocks simulated from the computation of the mapped and simulated four fracture sets. This is not a good representation of fractures of the research area. The poor representation is attributed to including of the deterministic Fracture Set 4 (bedding planes) in the computation. Bedding planes dip into the open pit wall, as thus this set does not contribute to the formation of blocks. Also, the mine is in a sedimentary terrain, therefore all other mapped fractures are younger and cut the bedding. Thus, it is believed that failures occur to expose the bedding. Bedding planes

are not failure release planes, they are exposed only after failure due to the interaction of the other three fracture sets.

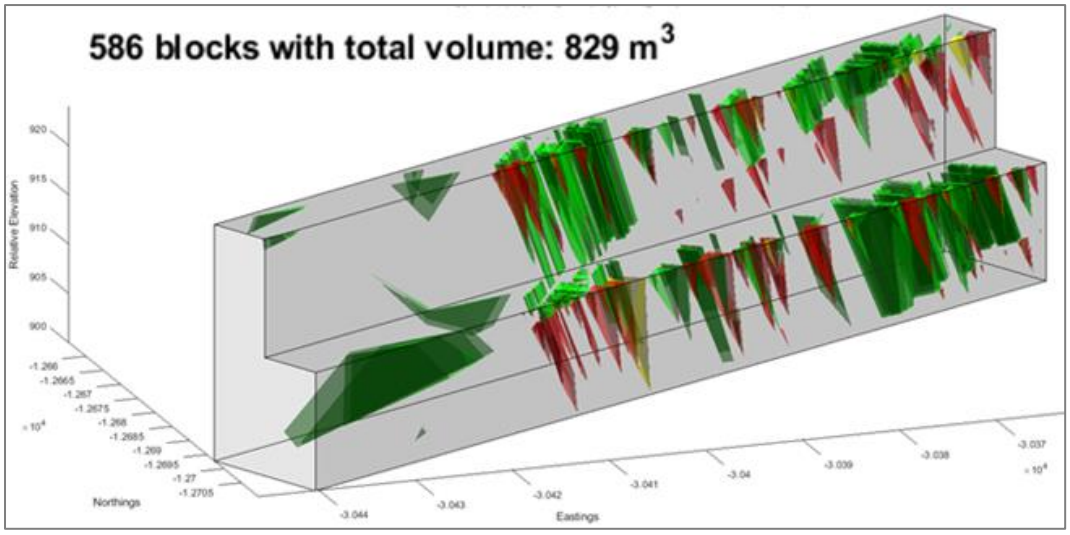


Figure 27: Block simulated from the four mapped fracture sets

An acceptable representation of field observed blocks was achieved by only utilising the three stochastic fracture sets as shown in Figure 28. One hundred Monte Carlo simulations were run using this scenario and the results are discussed in the following sections.

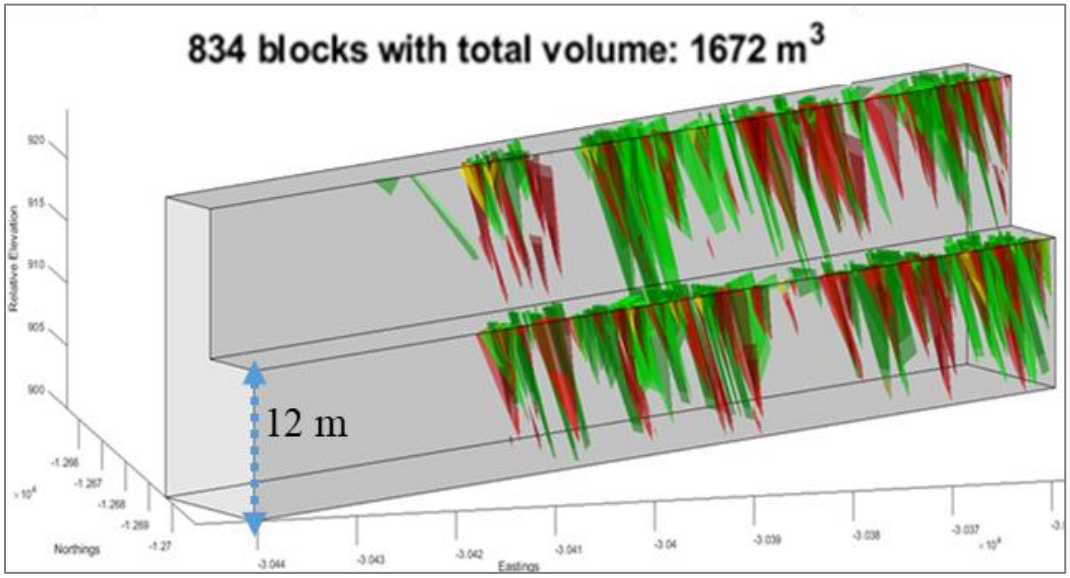


Figure 28: Block model simulations from the three stochastic fracture sets

6.1 Block Model Analysis

This section presents and analyses statistics from one hundred Monte Carlo simulations.

6.1.1 Effective Face Angle

From Figure 29, it is observed that 100% of the bench face fails at the current 90° design angle. The figure also shows that at 75° all bench faces are stable and this suggests that 75° is the optimum face angle for the research area.

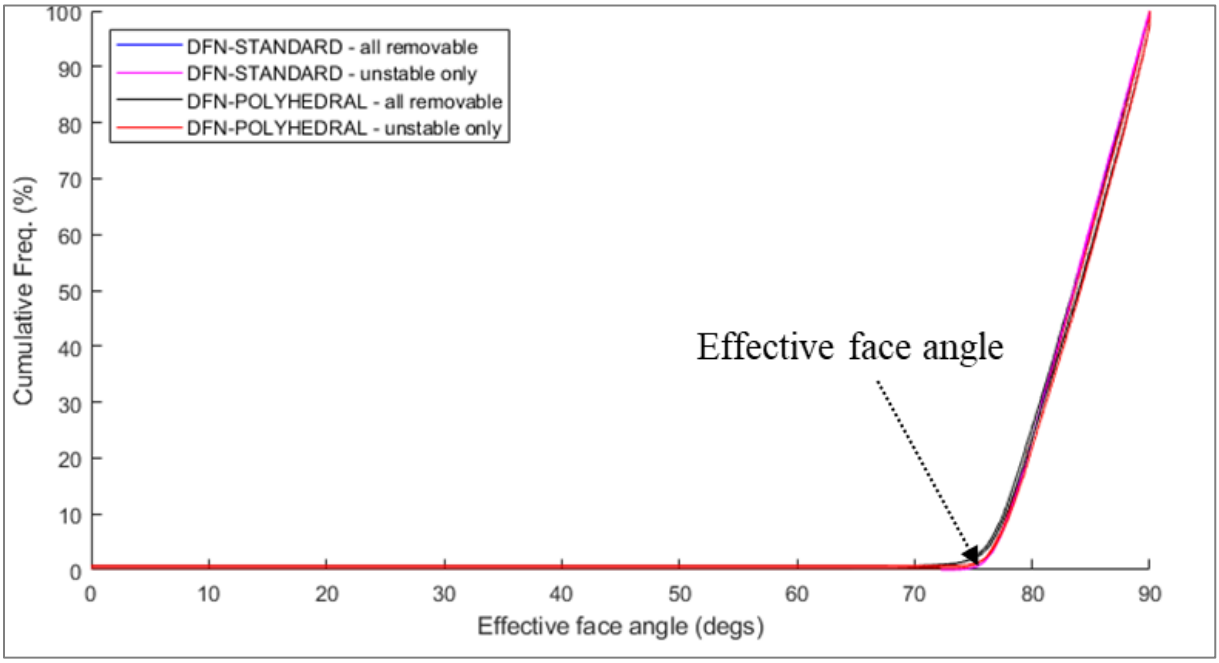


Figure 29: Effective face angle analysis of the research area

6.1.2 Back Break Analysis

Figure 30(a) shows that the research area will experience a maximum back break of 3 m wide with the current bench design of 90°. Associated with these back breaks, individual event/occurrence of rockfall incidents will have a modal strike length of 8 m as shown in Figure 30(b).

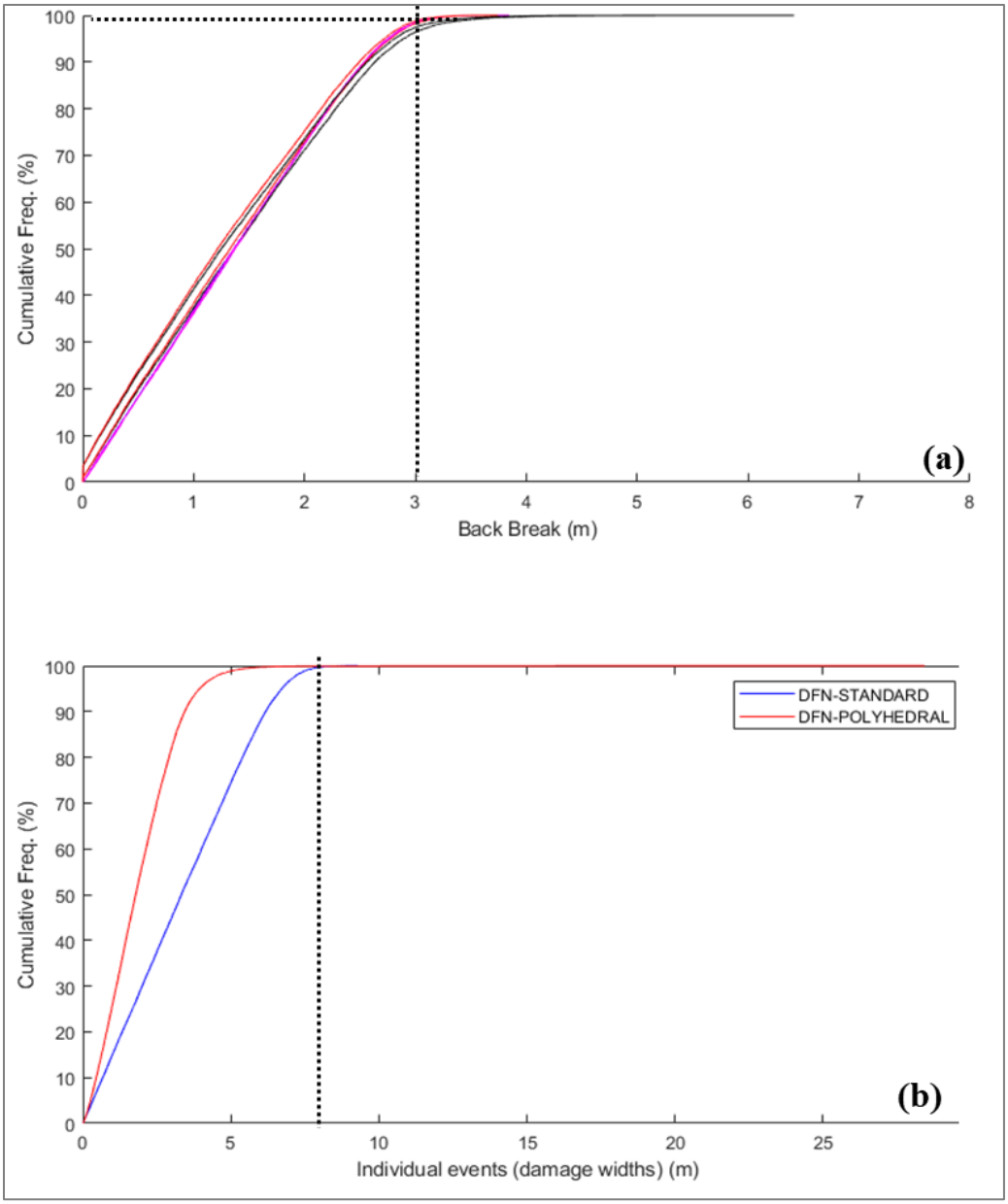


Figure 30: Back break analysis of the research area (a) Back break analysis (b) Individual events strike length analysis

6.1.3 Crest Damage Analysis

Expected crest damage is defined by the interaction of the various Fracture sets with the open pit geometry. Field observations indicate that crest loss must be expected in almost the whole length of the research area. Figure 31, from SiroModel simulations corroborates the expected crest damage as observed in the field.

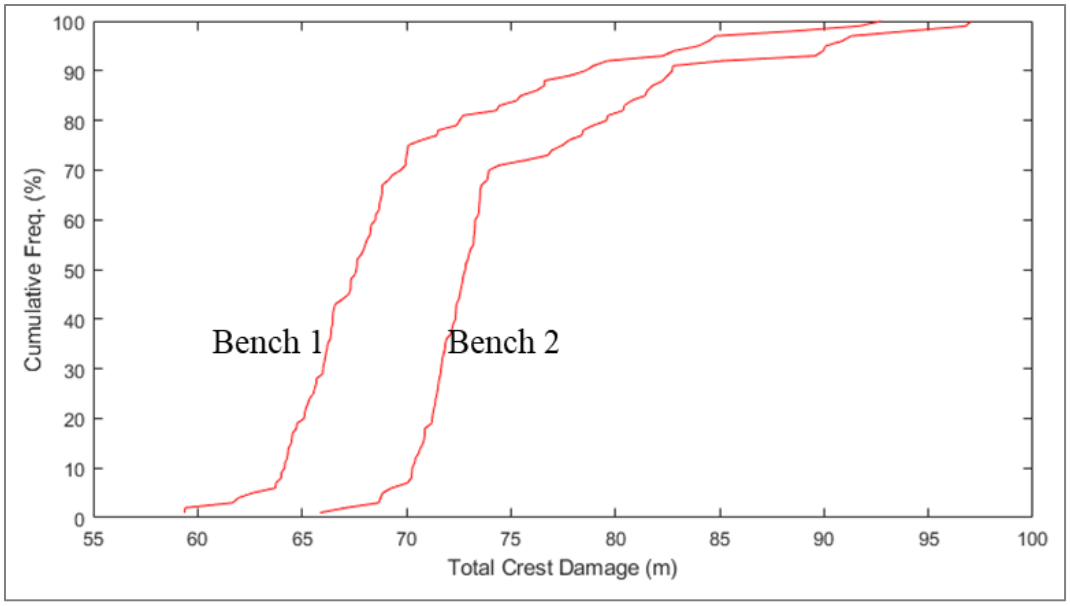


Figure 31: Total crest damage analysis (along the strike length)

6.1.4 **Block Volume Analysis**

The block volume analysis of the research area is shown in Figure 32.

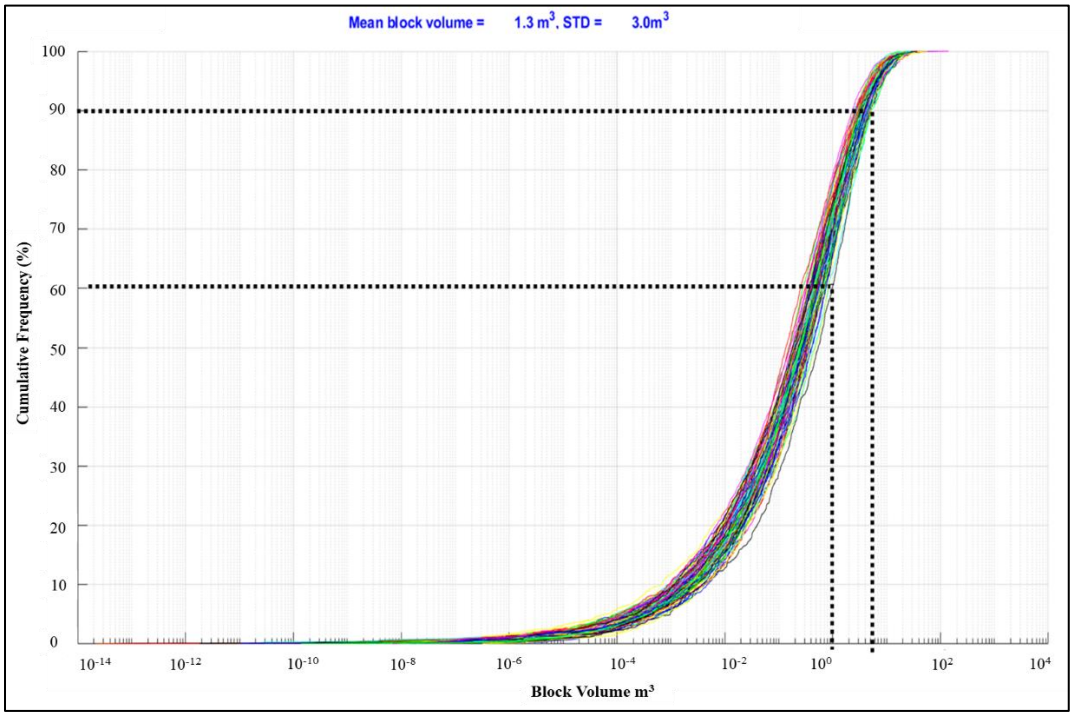


Figure 32: Potential rockfall block volume distribution within the study area

This figure shows that 1.3 m^3 is the mean volume of the potential rockfalls, with a standard deviation of 3 m^3. About 60% of the expected volume of rockfalls will be 1 m^3 or less. 30% of the potential rockfalls will have volumes range of 1 m^3 to 10 m^3. Only 10% of the potential rockfalls are predicted to have volumes greater than 10 m^3. These observations agree with the field observations. Also this is the expectation from the kinematic analysis of the fractures that form wedges. The fractures that form wedges are steeply dipping (see fracture sets 1, 2 & 3 in Table 3). Steeply dipping fracture sets that intersect to form a wedge release little material on failure. Steeply dipping fractures define small wedge; therefore little material is available for release during failure.

Block volume analysis coupled with block location analysis and hazard map analysis are critical parameters for recommendations on operational controls and mitigations. These recommendations are valuable to geotechnical clients such as the mining team. These parameters (block volume analysis coupled with block location analysis and the hazard map) allow the mining team to be aware of locations and sizes of potential rockfalls, thereby proactively plan mitigation measures to minimise negative impact on mining schedules. The proactive mitigation also ensures reduced levels of rockfall risk to personnel and equipment. The block volume analysis coupled with block location analysis is shown in Figure 33 and the hazard map analysis is shown in Figure 34.

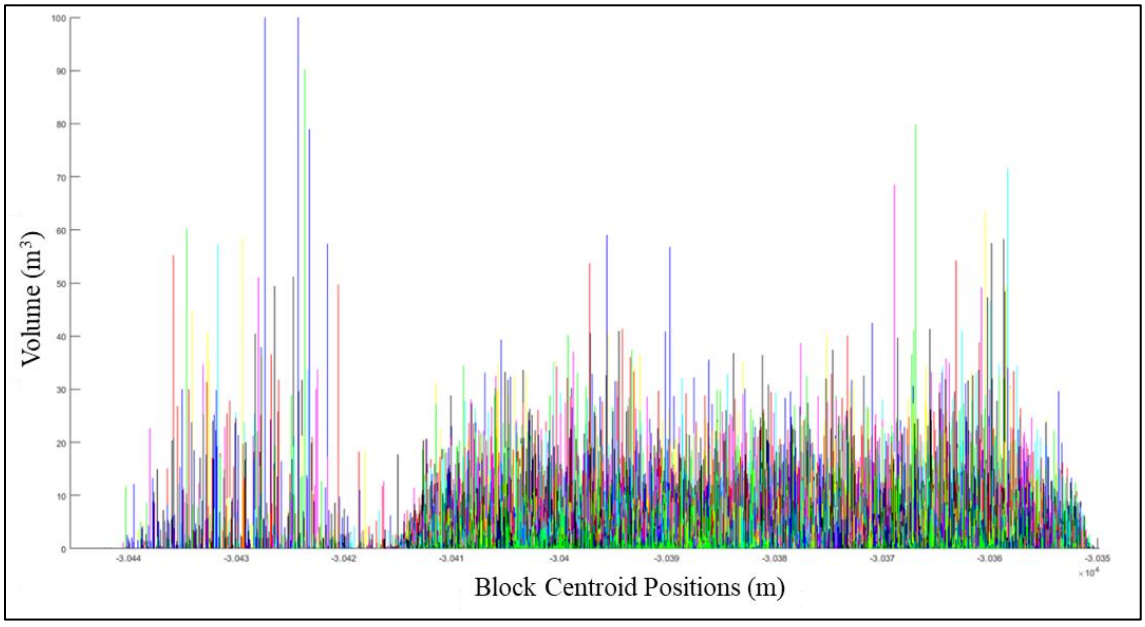


Figure 33: Block location analysis of the 100 Monte Carlo simulations

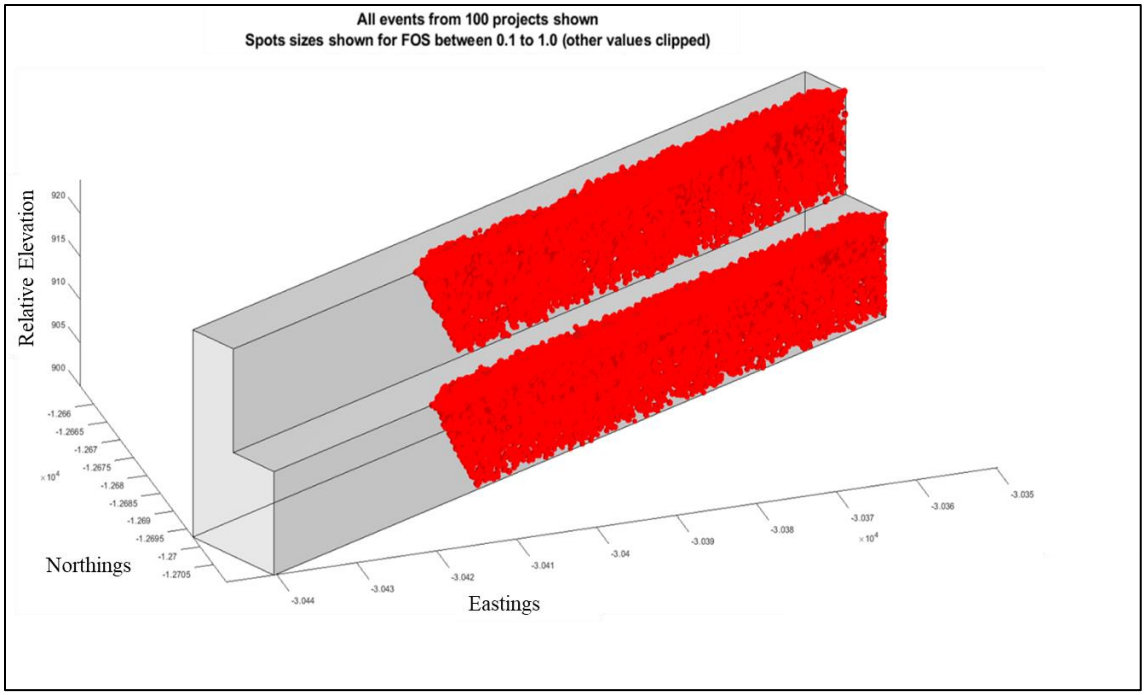


Figure 34: Potential rockfall Hazard Map of the research area

6.2 Chapter summary

Chapter 6 presents the analysis of the block model statistics. The block model was built in SiroModel using 100 Monte Carlo simulations. It is worth noting that the current practice of using stereonet analysis at Jwaneng Mine does not have the capacity to do this block model analysis. The SiroModel block model enabled critical bench scale analysis of rockfalls by utilising bench parameters such as effective bench face angle, back break analysis, rockfall volumes and crest damage. SiroModel also provides important outputs for the Jwaneng mining team. Through the use of SiroModel, visual presentations of locations of potential rockfall risks are provided. These visual presentations greatly assist in placing recommended operational controls for the identified risks.

7 CONCLUSIONS AND RECOMMENDATIONS

7.1 Conclusions

The current bench design angle of 90° is sub-optimal for the study area. At a 90° bench face, there is an elevated risk of rockfalls and total crest damage. The potential rockfalls have mean volume of 1.3m^3. This rockfall volume cannot be contained on the bench catchment because they occur on the crest side of the bench. Post the loss of the crest, the remain bench catchment width is becomes inadequate in achievement of control and management of 85% of rockfalls as per the Large Open Pit standard to which Jwaneng Mine is a member. It is therefore concluded that the 90° bench face angle introduces unacceptable risk to Jwaneng Mine, a company that ascribes to zero (0) harm. There is need to review, with the aim of reducing the bench face angle design. For the research area as demonstrated in previous chapter, 75° bench face angle is the optimal bench face angle. At 75°, the risks of rockfalls will be reduced to as low as reasonably possible which will have a net positive effects on the following mining and business aspects;

- Low risk of personnel injury and equipment damage: Low occurrence of rockfalls as a result of bench face angle optimization means limited opportunity of exposure for people and machinery. However, it must be noted that the low occurrence des not reduce the consequence when the risk is realized; a rockfall occur.

- Improved cycle times: During rainy seasons, when rockfall risk is further elevated by water on rocks, Jwaneng Mine haul ramps are converted into single access ramps. This means haul trucks use longer routes to take material out of the pit.

- Improved reputation: all mines, both open pit and underground continually battle with rockfall related incidents. This bench face angle optimization will thrust Jwaneng Mine into market leader and bench mark on addressing rockfalls.

SiroModel is an acceptable software for rockfall analysis in the Jwaneng Mine. Although SiroModel cannot analyse flexural toppling, this does not nullify the use of the software in Jwaneng Mine because flexural toppling is not the primary mode of failure of concern in Jwaneng Mine.

Jwaneng Mine currently uses RocScience Dips stereoplots for kinematic analysis. However, SiroModel is a superior tool to the stereoplot for rockfall analysis. SiroModel creates many realisations/simulations of DFNs by utilising the Monte Carlo simulation, therefore it is statistically representative and offers the best opportunity for producing near-real life representation of the dynamic anisotropic rockmasses in which mining operations occur. It is worth noting that stereoplot data is a critical input to DFN modelling because it offers a simple and easy way of statistically sorting Fracture sets data. Comparisons between SiroModel and the stereoplot are only possible at calibration stage of the DFN model. The stereoplot does not have the capability of producing similar outcomes as DFN modelling. DFN model outputs that are not available on the stereoplot include effective face angle, back break and block volume analysis. These outputs are critical to operational decision making which further proves the superiority of SiroModel for rockfall analysis

7.2 Recommendations

The research was undertaken on Cut 7 open pit walls with the objective of applying the results on Cut 9 open pit walls. This extrapolated application of results is possible and acceptable because it was proven that theses open pit walls have similar have the similar geological structural fabric. As discussed in the conclusions, it is recommended that Jwaneng Mine design optimal bench configurations by ensuring alignment with kinematic analysis. For the research area, a bench face angle of 75° is recommended because it reduces risk of rockfall occurrence to an as low as reasonably possible state. The extent of the research area is a 100m length over 24m height. This research must extended to ensure its representative of the rest of Cut 9 before it is fully implemented.

A comprehensive trade-off profit-loss studies of safety versus economic gain need to be completed before the 75° bench face angle is adopted. The bench face angle of 75° is considerably shallower than the current 90°. Designing shallower bench face angle has a cumulative shallowing effect on the inter-ramp and overall slope angles. Open pit mines with shallower overall slope angles have a limited depth to which they can be mined and therefore reach end of life faster. Jwaneng Mine

exploits vertical kimberlite pipes, this means volume of kimberlite and by extension diamonds that may be extracted at the reduced bench face angle will reduce considerably.

Double and/or triple bench configurations represents opportunities to optimise bench face angles with minimum change to the inter-ramp and overall slope angle. Legislations need to be taken into account when implementing such mining configurations. Use of SiroModel is recommended in investigating Double and/or triple bench configurations for Cut 9 open pit walls.

8 REFERENCES

Adhikary, D.P., Elmouttie, M., Lemiale, V. & Poulsen, B. 2016. Recent advances in the stability assessment of natural & engineered rock slopes. Journal of Nepal Geological Society, Vol. 50, pp. 65-72.

Adhikary, D. P., Dyskin, A. V., Jewell, R. J. & Stewart. D. P. 1997. A Study of the Mechanism of Flexural Toppling Failure of Rock Slopes. Rock Mechanics & Rock Engineering, 30 (2), 75-93.

Balzarini, M., Nicula, S., Mattiello, D. & Aliverti, E., 2001. Quantification & description of fracture network by MRI image analysis. Magnetic Resonance Imaging,19 (3-4) pp. 539 - 541.

Barnett, W., 2008. Jwaneng Country Rock Model prepared for Jwaneng Mine. Vancouver: SRK consulting engineers & scientists.

Brideau, M.A., Yan, M. & Stead, D., 2009. The role of tectonic damage & brittle rock fracture in the development of large rock slope failures. Geomorphology, 103(1), pp. 30-49.

Creus, P.K., Basson I.J., Stoch, B., Mogorosi. O., Gabanakgosi, K. & Ramsden F., 2018. Structural analysis & implicit 3D modelling of Jwaneng Mine: Insights into deformation of the Transvaal Supergroup in SE Botswana. Journal of African Earth Sciences, I (137), pp. 9-21.

CSIRO, 2019. SiroModel e-manuals. Available at: http://www.csiro.au/3dvision/SiroModel/e-Manuals/OPSMain.htm [Accessed 04 October 2019].

Debswana, 2017. Jwaneng Mine Internal reports. Jwaneng: Debswana Jwaneng Mine.

Debswana, 2018. Debswana Diamond Company – Jwaneng Mine Operation. Available at: http://www.debswana.com/Pages/default.aspx.Online [Accessed 12 February 2018].

Dershowitz, W.S. & Einstein, H.H. 1988. Characterizing rock joint geometry with joint system models. Rock Mechanics & Rock Engineering, Vol. 21, No. 1: 21-51.

Dershowitz, W.S. & Herda, H.H. 1992. Interpretation of fracture spacing & intensity. American Rock Mechanics Association. The 33rd U.S. Symposium on Rock Mechanics, 3 – 5 June, Santa Fe

Dirks, P.H.G.M., 2001. An investigation of the main fault planes in & near the open pit at Jwaneng Mine, Botswana; Development of a 3-D structural model for pit design purposes. Report Number Dirks 512TL, SRK Zimbabwe, 56p.

Elmo, D., Liu, Y. & Rogers, S., 2014. Principles of discrete fracture network modelling for geotechnical applications. Proceedings of DFNE2014 – 1st International Conference on Discrete Fracture Network Engineering, 19 –22 October, Vancouver.

Elmo, D., Stead, D. & Rogers, S., 2015. Guidelines for the quantitative description of discontinuities for use in discrete fracture network modelling. International Society for Rock Mechanics & Rock Engineering, 2015.

Elmouttie, M., Poropat, G. & Krähenbühl, G. 2010. Polyhedral modelling of rock mass structure. International Journal of Rock Mechanics & Mining Sciences, Vol. 47, No. 4: 544 – 552.

Elmouttie, M. & Karekal, S. 2017. A Framework for Geotechnical Hazard Analysis in Highwall Mining Entries. Symposium of the International Society for Rock Mechanics, 191: 1203 – 1210

Grenon, M., L&ry, A., Hadjigeorgiou. J. & Lajoie. P.L. 2016 Discrete fracture network based drift stability at the Éléonore mine. Mining Technology, 126:1, pp. 22 – 33.

Griffith, W., 2009. Influence of outcrop scale fractures on the effective stiffness of fault damage zone rocks. Pure & Applied Geophysics, 166(10-11), pp.1595-627.

ISRM (1981). International Society Rock Mechanics suggested methods for rock characterization testing & monitoring. Brown, E T Editor Imprint Oxford: Pergamon.

Jambayev, A., 2013, Discret Fracture Network for Modelling Carbonate Reservoir

Jing, L. & Stephason, O., 2007. Fundamentals of discrete element methods for rock engineering theory & applications. Potsdam, Germany: Elsevier.

Jones, R., Pearce, M.A., Jacquelyn, & Watson, F.E., 2016. Robust best-fit planes from geospatial data. Geosphere, 12(1), pp.196-202.

Lei, Q., Latham, J.P. & Tsang, C., 2017. The use of discrete fracture networks for modelling coupled geomechanical & hydrological behavior of fractured rocks. Computers & Geotechnics, 85, pp. 151 - 176.

Mapeo, R.B.M. & Wingate, M.T.D., 2009. SHRIMP U–Pb zircon age for the Segwagwa–Masoke Igneous Complex of southeastern Botswana & implications for the deformation history of the Achaean to Proterozoic Transvaal Supergroup of southern Africa. Journal of African Earth Sciences, 1(54), pp. 97-106.

Mathis, J.I., 2014. To DFN or not DFN - a question of circumstances. Proceedings of DFNE 2014 – 1st International Conference on Discrete Fracture Network Engineering, 19 –22 October, Vancouver.

Mauldon, M. 1998. Estimating Mean Fracture Trace Length & Density from Observations in Convex Windows. Rock Mechanics & Rock Engineering, 31, pp. 201 – 216.

Mauldon, M. & Wang, X. 2006. Proportional errors of the Terzaghi correction factor. American Rock Mechanics Association. The 41st U.S. Symposium on Rock Mechanics, Colorado.

Miyoshi, T., Elmo, D. & Rogers, S., 2017. Influence of Data Characterization Process on the Kinematic Stability Analysis of Engineered Slopes using Discrete Fracture Network Models. Proceedings of the 15th IACMAG, Wuhan.

Moore, J.M., Tsikos, H. & Polteau, S., 2001. Deconstructing the Transvaal Supergroup, South Africa: Implications for Palaeoproterozoic palaeoclimate models. Journal of African Earth Sciences, 1(33), pp. 437-44.

Pointe R.P., Wallmann, P. & Dershowitz. W.S. 1993. Stochastic Estimation of Fracture Size Through Simulated Sampling. Rock Mechanics & Mining Sciences & Geomechanics Abstracts, 30 (7), pp. 1611 – 1617.

Pollard, D.D. & Segall, P., 1987. Theoretical displacements & stresses near fractures in rock: with application to faults, joints, veins, dikes & solution surfaces. In B.K. Atkison, ed. Fracture mechanisms of rock. London: Elsevier Ltd. pp. 277-349.

Priest, S.D. 1993. Discontinuity analysis for rock engineering. Chapman & Hall, Hong Kong.

Read, J. & Stacey, P. (Eds.), 2009. Guidelines for Open Pit Slope Design. CSIRO Publishing, Collingwood.

Ryan, T.M. & Pryor, P.R., 2000. Designing catch benches & inter ramp slopes. Slope Stability in Surface Mining. SME, Littleton, Colorado. pp. 27-38.

Staub. I., Fredriksson, A., Outters, N. & Golder Associates AB. 2002. Strategy for a Rock Mechanics Site Descriptive Model: Development & testing of the theoretical approach. SKB Report, R02-02. Swedish Nuclear Fuel & Waste Management, Stockholm

Terzaghi, R.D. 1965. Sources of Error in Joint Surveys. Geotechnique, 15(3), pp. 287 – 304.

Thoeni, K., Giacomini, A., Sloan, S.W., Lambert, C. & Casagr&e, D., 2011. Numerical analysis of rockfall hazard in open pit coal mines. Proceedings of 13th International Conference of the International Association for Computer Methods & Advances in Geomechanics, IACMAG 2011; Melbourne, VIC; Australia; 9 – 11 May. 2(I), pp. 1151-1156.

Warburton, P.M. 1980. Stereological Interpretation of Joint Trace Data: Influence of Joint Shape & Implications for Geological Surveys. Rock Mechanics & Mining Sciences & Geomechanics Abstracts, 17(6), pp. 305 – 316.

Wyllie, D.C. & Mah C.W. 2004. Rock Slope Engineering Civil & Mining, 4th edition. Spon Press, London and New York.

Xu, C. & Dowd, P., 2010. A new computer code for discrete fracture network modelling. Computers & Geosciences, 36, pp. 292-301

Zhang, L. & Einstein, H.H. 2000. Estimating the intensity of rock discontinuities. Rock Mechanics & Mining Sciences, 37, pp. 819 – 837.